Title: Enhanced protective efficacy of a novel, thermostable, RBD-S2 fusion immunogen against SARS-CoV-2 and its variants

Authors: Nidhi Mittal[1], Sahil Kumar[2], Raju S Rajmani[1], Randhir Singh[3], Céline Lemoine[4], Virginie Jakob[4], Sowrabha BJ[3], Madhuraj Bhat[3], Debajyoti Chakraborty[1], Suman Pandey[3], Aurélie Jory[5], Suba Soundarya S.A.[5], Harry Kleanthous[6], Patrice Dubois[4], Rajesh P. Ringe[2*], Raghavan Varadarajan[1*]

Affiliations:

[1]Molecular Biophysics Unit (MBU), Indian Institute of Science, Bengaluru 560012, India

[2]Virology Unit, Institute of Microbial Technology, Council of Scientific and Industrial Research (CSIR), Chandigarh 160036, India

[3]Mynvax Private Limited, 3rd Floor, Brigade MLR Centre, No. 50, Vani Vilas Road, Basavanagudi, Bengaluru 560004, India

[4]Vaccine Formulation Institute, Rue du Champ-Blanchod 4, 1228 Plan-les-Ouates, Switzerland

[5]National Centre for Biological Sciences, Tata Institute of Fundamental Research, Bengaluru 560065, India

[6]Bill and Melinda Gates Foundation, Seattle, WA, 98109, USA

*Corresponding authors: rajeshringe@imtech.res.in varadar@iisc.ac.in

Abstract: With the rapid emergence of variants of concern (VOC), the efficacy of currently licensed vaccines has reduced drastically. VOC mutations largely occur in the S1 subunit of Spike. The S2 subunit of SARS-CoV-2 is conserved and thus more likely to elicit broadly protective antibody and T-cell responses. However, the contribution of the S2 subunit in improving the overall efficacy of vaccines remains unclear. Therefore, we designed, characterized, and evaluated the immunogenicity and protective potential of a stabilized SARS-CoV-2 Receptor Binding Domain (RBD) fused to a stabilized S2. Designed immunogens were expressed as soluble proteins with significantly higher purified yield than the Spike ectodomain. Squalene-in-water emulsion (SWE) formulated fusions were highly immunogenic. S2 immunization failed to elicit a neutralizing immune response but significantly reduced lung viral titers in mice challenged with the heterologous Beta variant, while RBD-S2 fusions elicited broad neutralization including against the Clade 1a WIV-1 variant, and were highly efficacious. A lyophilized RBD-S2 fusion retained antigenicity and immunogenicity even after incubation at 37 °C for a month. In hamsters, SWE-formulated RBD-S2 showed enhanced immunogenicity and efficacy relative to corresponding RBD and Spike formulations.

Keywords: Thermostable, protein engineering, lyophilization, potency, protein design

Introduction

The severe acute respiratory syndrome coronavirus 2 (SARS-CoV-2) virus is the causative agent of the COVID-19 pandemic *(1)*. A variety of SARS-CoV-2 vaccines were developed at an unprecedented pace to combat the pandemic *(2–10)*. Spike (S) is a ~ 200 kDa transmembrane glycoprotein composed of two functional subunits: the N-terminal S1 subunit, which mediates attachment to the host receptors, and the C-terminal S2 subunit, which facilitates membrane fusion *(11–13)*. Spike protein is highly immunogenic, and the receptor-binding domain (RBD) contains the major neutralizing antibody epitopes *(14–20)*. Most currently approved vaccines are based on the Spike immunogen, and a minority are based on RBD. RBD-based vaccines have been shown to elicit moderate to high-neutralizing antibody titers *(21–24)*. However, due to rapid virus evolution, various variants of concern (VOC) mutations have been identified primarily in the N-terminal domain (NTD) and RBD of the S1 subunit *(25)*. These mutations increase viral infectivity and induce immune evasion by evading virus neutralization. Requirements for low or ultracold temperature storage have acted as barriers to vaccine deployment in low-and middle-income countries (LMICs). Therefore, there is an imperative need for vaccine candidates that confer a potent, protective, humoral immune response to a broad spectrum of SARS-CoV-2 variants and do not require a cold-chain for last mile distribution.

Compared to the S1 subunit, the S2 subunit of coronaviruses is more conserved and likely to elicit broadly protective antibodies *(26)*. Several cross-reactive monoclonal antibodies against the S2 stem helix region have been identified, and a few of them have been shown to neutralize SARS-CoV-2, thereby conferring *in vivo* protection *(19, 27–36)*. Spike microarray analysis demonstrated that cross-reactive antibodies are elicited against the S2 stem helix region during natural infection *(19)*. The stem-helix epitope in the S2 region, residues (1142-1165) is well conserved, and antibodies that bind to this region neutralize diverse coronaviruses suggesting that immunogens containing this cryptic epitope might elicit pan-coronavirus immunity.

However, the protective efficacy of S2 as an immunogen remains unclear. It is also known that the bulk of the neutralizing response is directed against the RBD. While there are also neutralizing antibodies directed against the N-terminal domain (NTD) of the Spike, these have lower breadth than the RBD-directed neutralizing antibodies, as the major NTD neutralizing epitope is mutated in VOCs *(37–41)* To address these issues, we designed S2-ectodomain, RBD-S2, and S2-RBD fusion-based immunogens. Designed immunogens were recombinantly expressed in mammalian

cells and purified at higher yields. Two immunizations of Sepivac SWE™ (further referred to as SWE)-formulated RBD-S2 immunogen induced robust neutralizing immune responses and conferred protection against SARS-CoV-2 variants in mice and hamsters. Although no neutralization was seen in mice immunized with SWE formulated S2 (lacking RBD), following challenge, lung viral titers were significantly reduced in this group also, relative to unimmunized controls. Comparative studies with a stabilized Spike ectodomain revealed that RBD-S2 was expressed with ~5.3-fold higher purified yield and showed superior immunogenicity and protective efficacy in hamsters.

Results

Immunogen Design

For designing an S2-based SARS-CoV-2 immunogen, S2 subunit residues interacting with the S1 subunit were identified by accessibility calculations using the Naccess program on PDB 6VXX. Accessible surface areas (ASA) of all residues in the Spike were calculated in the absence and presence of the S1subunit. Residues of the S2, which had a total side-chain ASA difference of >5 $Å^2$, were identified as S1 interacting residues. The following mutations were made to mask newly exposed hydrophobic residues to prevent S2 aggregation in the absence of S1, namely F855S, L861E, L864D, V976D, and L984Q *(42, 43)*.

Proline substitutions in the loop between HR1 (heptad repeat 1) and the central helix in fusion proteins from viruses like SARS-CoV-2, SARS-CoV, MERS-CoV, and RSV are known to destabilize the postfusion conformation, and enhance expression yields *(44–47)*. More recently, HexaPro Spike, a S-6P variant, with six proline substitutions (F817P, A892P, A899P, A942P, K986P, V987P) displayed 9.8-fold increased protein expression and ~5 °C increase in T_m relative to S-2P *(48)*. Hence, we additionally included all these six proline substitutions in the present S2 immunogen (S2) comprising residues 698-1211 of the SARS-CoV-2 Spike.

Since RBD contains the major neutralizing antibody epitopes on Spike and S2 is well conserved, we designed RBD-S2 fusion immunogens. For this, an S2 fragment comprising residues 698-1163 of the SARS-CoV-2 was genetically fused with our previously reported high-yielding, thermostable RBD containing A348P, Y365W, and P527L mutations *(22, 24)*. Two variants of RBD-S2 fusion constructs, RS2 and S2R, were constructed **(Fig. 1A)**.

Biophysical characterization of S2, RBD-S2 and S2-RBDfusion immunogens

The designed immunogens were transiently expressed as secreted proteins in Expi293F suspension cells. Recombinant proteins S2, RS2, and S2R were purified in high yields of ~120 mg/L, ~850 mg/L, and ~800 mg/L, respectively, using nickel affinity chromatography **(Fig. 1B)**. RBD-S2 fusions, RS2 and S2R, exhibited ~5.3-fold higher protein yields than Spike. The oligomeric state of the immunogens was determined using size exclusion chromatography- multi-angle light scattering (SEC-MALS), and revealed that RBD-S2 fusion immunogens RS2 and S2R exist as a mixture of monomers and trimers **(Fig. 1D, E)**. S2 exists as homogenous nonamers in the solution, and the calculated molecular weights were in good agreement with the theoretical molecular weight **(Fig. 1C)**. RS2 and S2R have similar thermal unfolding profiles and comparable melting temperatures (T_m ~ 50 °C) **(Fig. 2B-C)**. Compared to S2R, RS2 is more rapidly digested by TPCK-trypsin at 4 °C and 37 °C **(Fig. 2E and F)**. The stabilized S2 immunogen (S2) has an apparent melting temperature (T_m) of 52.2 °C and shows slightly more resistance to trypsin proteolysis at both 4 °C and 37 °C than RBD-S2 fusion immunogens. Thus, the addition of S2 to RBD results in decreased thermal and proteolytic stability of S2 and RBD **(Fig. 2A and D)** *(22, 24)*. The binding of S2, RS2, and S2R immunogens to its cognate receptor, ACE2-hFc, a panel of RBD conformation-specific (CR3022, S309, ADG-2, and H014) and S2-specific (B6 and CC40.8) antibodies were probed using surface plasmon resonance. Spike, RS2, and S2R bind well with ACE2-hFc, RBD-specific, and S2-specific antibodies (**Fig. 3 and 4) (Table S1 and S2)**. S2 binds only to S2-specific antibodies with high affinity. This indicates the proper folding of designed immunogens **(Fig. 4) (Table S2)**.

Low-dose RS2 immunization protects mice against mouse-adapted SARS-CoV-2 challenge.

The relative ability of the RBD-S2 fusion immunogen, RS2, to induce neutralizing antibody titers at a standard dose (20 μg) and a 10-fold lower dose (2 μg) was assessed. Female BALB/c mice were intramuscularly immunized at week 0 and week 3 with either 2 or 20 μg of RS2 immunogen formulated with SWE. Both vaccine doses (2 and 20 μg) elicited comparable RBD and Spike-specific IgG titers and neutralizing antibody titers against wild-type (B.1), Delta, BA.1, and BA.5 Omicron pseudoviruses **(Fig. S1A-H)**. Results suggest that a 10-fold reduction in the vaccine dose does not compromise the neutralizing immune response. Three weeks post-boost, all mice were intranasally challenged with 10^5 plaque-forming units (pfu) of mouse-adapted SARS-CoV-2 MA10 virus. One-day post-challenge, mice immunized with either 2 or 20 μg of RS2 showed a

slight body weight reduction of ~5 %, and from day two, all mice regained their initial weight. In contrast, unimmunized-virus challenge control (VC) mice showed ~25 % weight loss by day four, post-challenge **(Fig. S1K)**. RS2 also elicited substantial cross-neutralization against heterologous clade1a WIV-1 virus, which demonstrates the potential of RBD-S2 to elicit broadly protective antibodies against sarbecoviruses **(Fig. S1I)**. Analysis of lung tissue sections of mice immunized with 2 μg of RS2 showed clear lung epithelial interstitial spaces and lower immune cell infiltration compared to virus challenged group (data not shown). This data suggests that RS2 elicits a good humoral immune response and protects against the SARS-CoV-2 MA10 virus challenge. A lower 2 μg dose also elicits comparable protection to the 20 μg dose.

Immunogenicity and protective efficacy of S2R relative to S2 and RBD immunogens against heterologous challenge.

The immunogenicity of RBD-S2 fusion immunogen, relative to RBD and S2 immunogen, was evaluated in hACE-2 expressing C57BL/6 transgenic mice. Our previously reported mammalian cell expressed, stabilized RBD containing A348P, Y365W, and P527L mutations was expressed and purified *(22, 24)*. Mice were intramuscularly immunized with 2 μg immunogens (S2R, S2 or RBD) formulated with SWE in a prime-boost regimen 3 weeks apart. Two weeks post-boost, RBD and Spike-specific IgG titers in sera of immunized mice were measured using ELISA. Relative to RBD and S2, the S2R (RBD-S2 fusion) immunogen elicited significantly higher RBD and Spike-specific ELISA endpoint titers **(Fig. 5A and B)**. Both RBD and S2R immunized mice elicited high neutralizing antibody titers against B.1 pseudovirus **(Fig. 5C)**. S2R immunized mice showed significantly reduced neutralizing titers against BA.1 pseudovirus, while no neutralization against BA.1 was seen in RBD-immunized mice at this dose of immunogen **(Fig. 5D)**. Although mice immunized with the S2 immunogen failed to elicit a neutralizing immune response, the data shows that the inclusion of S2 can improve the immunogenicity of RBD-based vaccines **(Fig. 5C)**.

Next, the protective efficacy of RBD, S2, and S2R was assessed against the Beta variant of SARS-CoV-2. Unimmunized-unchallenged (UC) and unimmunized-virus-challenged (VC) mice were used as control groups. Three weeks post boost, mice were intranasally challenged with 10^5 pfu of Beta variant, and weight change was monitored for up to five days. Post-challenge, no weight change was seen in S2R immunized mice. Mice immunized with RBD, and S2 showed a

significant weight reduction of ~10 % and ~17 %, respectively. As expected, no weight reduction was observed in the unimmunized-unchallenged group, while 22-25 % weight reduction was seen in the unimmunized-virus-challenged group **(Fig. 5E)**. Mice immunized with either RBD, S2 or S2R showed significantly lower lung viral titers than unimmunized mice challenged with the Beta variant **(Fig. 5F)**. Despite lack of neutralization, lung viral titers were significantly reduced in the S2-immunized group, suggesting that S2 provides protection by non-neutralizing mechanisms. The lung tissue sections obtained from S2R immunized mice showed clear interstitial spaces within lung epithelium and reduced immune cell infiltration compared to unimmunized virus-challenged groups **(Fig. 5G and H)**.

RS2 induces an equivalent neutralizing immune response to Spike ectodomain in mice and protects against Beta variant challenge.

Considering that most currently licensed COVID-19 vaccines have the Spike as the sole immunogen, we compared the immunogenicity and protective efficacy of our RBD-S2 fusion (RS2) with the Spike ectodomain. The stabilized trimeric Spike ectodomain (1-1211) contains six proline mutations (F817P, A892P, A899P, A942P, K986P, and V987P), along with the additional three RBD stabilizing mutations (A348P, Y365W, and P527L) *(24, 48)*. Protein was expressed in Expi293F cells and purified. hACE-2 expressing C57BL/6 transgenic mice were intramuscularly immunized with 20 µg of RS2 or Spike formulated with SWE adjuvant in a prime-boost regimen 21 days apart. Fourteen days post-second immunization, both RS2, and Spike immunized mice elicited high RBD and Spike-specific IgG titers **(Fig. S2A and B)**. Neutralizing titers against B.1 and BA.1 variant pseudoviruses were comparable in both RS2 and Spike immunized groups at this antigen dose **(Fig. S2C-F)**. Twenty-one days following the boost immunization, mice were intranasally challenged with 10^5 pfu of Beta variant. No weight change was seen in either of the immunized groups and the unimmunized-unchallenged control group. Unimmunized virus challenged mice showed drastic weight reduction 5 days post-challenge **(Fig. S2H)**. In comparison to the unimmunized-challenged group, lung tissue sections of RS2 and Spike immunized mice showed only minor pathological signs and symptoms of infection **(Fig. S2I and J)**.

Thermal stability of RBD-S2 fusions

As with our previously reported RBD immunogens, our newly designed S2, RBD-S2, and S2-RBD fusion immunogens showed identical thermal unfolding profiles before and after lyophilization and solubilization, suggesting that lyophilization did not affect the thermal stability of these immunogens **(Fig. S3A-C)** *(22, 24)*. Further, the effect of transient thermal stress on the thermal stability of lyophilized RBD-S2 immunogens, RS2 and S2R, were studied by performing nano-DSF. Following incubation at different temperatures (4 °C, 37 °C, 50 °C, 70 °C and 90 °C) for 60 min, no change in thermal unfolding profiles was observed for both RS2 and S2R **(Fig. S4A and B)**. In addition, the antigenicity of RS2 and S2R was assessed by performing surface plasmon resonance (SPR) using a panel of RBD and S2-specific antibodies. Interestingly, following thermal stress both RS2 and S2R retained binding with the cognate receptor ACE2-hFc, RBD-specific antibodies (CR3022, S309), and S2-specific antibodies (B6, CC40.8). This suggests that RBD-S2 fusion immunogens are resistant to transient thermal stress **(Fig. S4C-L)**. The T_m and conformational integrity of lyophilized RS2 protein remained unchanged after a month of storage at 37 °C **(Fig. S3D and Fig. 6A-F) (Table S3)**. The stability of SWE adjuvanted RS2 in PBS buffer was also evaluated at 5 and 40 °C over a period of one month. Antigen integrity and physiochemical characterization of SWE adjuvanted RS2 formulations was carried out by performing ELISA, particle size, polydispersity, zeta potential, pH, osmolality and squalene content measurements. The RS2 formulation in SWE is stable at 5 and 40 °C in both polypropylene tubes and glass vials for at least one month **(Fig. 6G-Q)**.

Protective efficacy of lyophilized RBD-S2 formulation after month long storage at 37 °C

The immunogenicity of the lyophilized RS2 protein stored at 37 °C for a month was evaluated in hACE-2 expressing C57BL/6 transgenic mice. Mice were intramuscularly immunized with 20 μg immunogen extemporaneously formulated with SWE adjuvant in a prime-boost regimen. Two weeks following the boost, the formulation showed high RBD and Spike-specific binding titers, and neutralizing titers against B.1, Beta, Delta, and BA.1 pseudoviruses **(Fig. 7A-C)**. The above formulation elicited equivalent neutralization titers to a non-lyophilized freshly prepared RS2 formulation stored at 4 °C, against B.1 and BA.1 pseudoviruses **(Fig. 7D)**. Twenty-one days following the boost, mice were challenged with 10^4 pfu of Beta and Delta variants of SARS-CoV-2. None of the unimmunized control mice survived Beta variant challenge, while 57% of unimmunized control mice survived Delta variant challenge and the remaining mice showed 20

% weight loss nine days post-challenge **(Fig. 7F and G)**. In contrast, RS2 formulated with SWE immunized mice survived the Beta and Delta variant SARS-CoV-2 challenge and showed no weight loss **(Fig. 7E-G)**. Lung viral titers of RS2-immunized mice challenged with Beta and Delta variants were below the detection limit and lung tissues showed minimal pathology **(Fig. 7H-K).** Lung viral titers and tissue sections from the unimmunized mice challenged with the Beta variant were not examined because none of the mice survived. These findings indicate that RS2 is stable and immunogenic even after storage at 37 °C for at least one-month.

RS2 shows superior immunogenicity and protective efficacy to stabilized Spike ectodomain in hamsters.

Dose sparing and protective efficacy of RS2 against the Beta variant of SARS-CoV-2 in Syrian hamsters was evaluated. Female Syrian Golden Hamsters were immunized with either a 5 or 20 μg dose of RS2 formulated with SWE on day 0 and day 21, while the control group of hamsters was immunized with PBS and SWE adjuvant **(Fig. S5)**. Both 5 and 20 μg doses induced strong RBD and Spike-specific IgG immune responses **(Fig. S5A and B)**. High neutralizing antibody titers were observed against B.1, Beta, and Delta variants of concern **(Fig. S5C-E)**. While a decrease in neutralizing titer was observed against the BA.1 variant for both dose groups, the titers were still significant, with a GMT of 688 and 306 for low and high dose groups, respectively **(Fig. S5G)**. Hamsters immunized with either dose of RS2 were protected against 10^5 pfu SARS-CoV-2 Beta variant challenge. Animals immunized with a lower dose showed lower weight loss and lower lung viral titers **(Fig. S5H and I)**. The unimmunized hamsters challenged with the Beta variant of SARS-CoV-2 showed significantly higher weight loss (~ 15 %) **(Fig. S5H)**. Lung tissue sections obtained from both 5 μg and 20 μg of RS2 immunized hamsters showed clear lung epithelial interstitial spaces and lower immune cell infiltration compared to unimmunized virus-challenged groups **(Fig. S5J and K**).

We also compared the protective efficacy of RS2 with the stabilized Spike in hamsters. Syrian hamsters were immunized with either 5μg of stabilized Spike formulated with SWE on day 0 and day 21. Notably, two immunizations with 5 μg SWE adjuvant formulated RS2 elicited significantly higher neutralizing titers against wild-type SARS-CoV-2, Beta, and Omicron BA.1 variants than SWE formulated Spike in hamsters **(Fig. 8A-G)**. Moreover, hamsters immunized with RS2 showed initial transient weight loss (up to 3 %) and regained weight at 3 days post-Beta variant infection. In contrast, Spike-immunized hamsters showed comparatively higher lung viral titers,

weight loss, while no weight regain was observed **(Fig. 8H and I)**. Both RS2 and Spike immunized hamsters showed significantly reduced lung viral titers compared to unimmunized and challenged hamsters **(Fig. 8H)**. Analysis of RS2 and Spike immunized hamster lung tissue sections showed clear lung epithelial interstitial spaces and lower immune cell infiltration compared to the unimmunized virus-challenged groups **(Fig. 8J and K)**. Overall, the data shows that RS2 is more immunogenic and efficacious than Spike in hamsters.

Discussion

Vaccination has significantly reduced the global health burden caused by the COVID-19 pandemic. While vaccines have been proven to be highly efficacious against ancestral SARS-CoV-2 stain, their efficacy has rapidly declined against new VOCs and periodic updating of vaccines appears to be necessary. Most VOC mutations are identified in the receptor binding motif (RBM) region of RBD. The substantial waning of serum-neutralizing antibody titers and the emergence of variants with increased transmissibility and neutralizing antibody escape responses are associated with increased breakthrough infection in vaccinated individuals. To curb infection and sustain vaccine effectiveness, booster doses are required. Mosaic nanoparticle vaccine designs, that display multiple RBD's from different sarbecoviruses, conferred broad protection against diverse coronaviruses, albeit with a reduction in potency against some SARS-CoV-2 VOCs *(49–51)* . However, these elicit titers against nanoparticle scaffolds, employ a large number of antigens, and this adds to manufacturing complexity. An alternative approach is to use conserved antigens for vaccine development. In an attempt to broaden the protection breadth of SARS-CoV-2 vaccines, we designed an S2 ectodomain and RBD-S2 fusion-based immunogens (RS2 and S2R). The RBD-S2 fusions contain the RBD component to elicit potent antibodies and the S2 to increase immunogenicity and protective breadth. The S2 component alone induced high IgG binding titers but sera failed to neutralize the virus. Despite lack of neutralization, lung viral titers were significantly reduced in S2 immunized mice compared to unimmunized Beta variant challenged mice in the present study, suggesting S2 directed antibodies can provides protection through non-neutralizing mechanisms likely involving Fc effector function. In an earlier study mice immunized with an S2 encoded DNA vaccine showed broad neutralization. In the same study boosting animals previously immunized with DNA encoded spike and boosted with S2 failed to protect against more Delta challenge *(52)*. In contrast bacterially expressed or insect cell line expressed S2 comprising of residues 686-1211 of the SARS-CoV-2 spike ectodomain elicited high Spike specific IgG titers

but no neutralizing titers against SARS-CoV-2 in mice and rabbits respectively *(52, 53)*. In a recent study, HR121, a recombinant subunit vaccine formulated with Freund's complete/ aluminium adjuvant elicited cross-neutralizing titers after three immunizations and protected hACE-2 Tg mice, hamsters and rhesus macaques against lethal SARS-CoV-2 challenge. Neutralizing antibodies target the HR2 binding to HR1, thus prevents membrane fusion and viral entry *(54)*. In another study, following three immunizations with an AS03 + pIC formulated MS2-VLP displaying S2, elicited sera neutralized B.1, Beta, Delta and BA.1 variants and vaccination significantly reduced viral titers in lungs and nasal turbinates after heterologous challenge *(55)*. However, yields were low and there are manufacturing challenges associated with this complex immunogen. In another report, double layered nanoparticles incorporating both prefusion Spike and S2 elicited significant neutralizing antibody titers, ADCC activity and cellular immune responses against pre-Omicron VOCs in mice but protective efficacy was not assessed *(56)*. In the present work the novel RS2 and S2R immunogens were expressed and purified from Expi293F cells at remarkably high yields. RS2 and S2R bound tightly to a panel of RBD-specific and S2-specific antibodies. In contrast to S2, both RS2 and S2R immunogens induced potent neutralizing antibodies against B.1, Beta, Delta, and Omicron (BA.1 and BA.5) pseudoviruses, protected mice against lethal challenge with SARS-CoV-2 and its Beta variant and showed enhanced immunogenicity and protective efficacy relative to the Spike ectodomain. Lyophilized RS2, even after incubation at 37 °C for a month, retained its thermal stability, antigenicity, immunogenicity, and protective efficacy. Encouragingly, physico-chemical stability and antigenicity of the RS2 immunogen formulated with SWE was also retained at 40°C for up to one month. SWE is equivalent to MF59, a very safe adjuvant that has been used for many years in the context of human influenza vaccines *(57)*. While there are other more potent adjuvants available, stronger adjuvant mediated immune responses can be associated with unfavorable side effects *(57)*. Previously, an RBD-HR chimeric ferritin nanoparticle vaccine elicited neutralizing titers comparable to an RBD-ferritin nanoparticle in mice but with broader cross-neutralization potential against other coronaviruses *(58)*. Another Ferritin displayed, alum adjuvanted Spike construct also displayed promising immunogenicity in non-human primates and could be stored at 37°C for at least two weeks *(59)*. The present RS2 immunogen elicited a significantly higher humoral immune response and protection against the Beta variant in hamsters compared to both the Spike ectodomain as well as RBD, the latter also required three immunizations in hamsters to elicit protective antibody titers

(24). RS2 also elicited cross-neutralizing antibody titers against the clade Ia WIV-1 virus. In addition, RS2 and S2R immunized mice sera showed good cross-reactivity with different sarbecovirus Spikes, suggesting that RBD-S2 fusion elicits higher cross-reactive antibodies than RBD, Spike ectodomain and S2 antigens **(Fig. S6)**. Whether the RBD-S2 fusion-based immunogen, RS2, protects against the broad range of sarbecoviruses needs to be further investigated. In future studies, cellular immune responses, effector function of S2 specific antibodies and the immunogenicity of RS2 will be further tested in NHP models. Overall, our data highlights the thermal tolerance of the RS2 adjuvanted formulation as well as the importance of S2 inclusion in RBD-based vaccine formulations to improve the immunogenicity and broaden the protective breadth of coronavirus vaccines.

Materials and methods

Expression and Purification of recombinant proteins

Recombinant proteins S2, RS2, S2R, RBD, and Spike were transiently expressed in Expi293F™ cells according to the manufacturer's guidelines (Gibco, ThermoFisher Scientific). Briefly, Expi293F™ cells were maintained at a cell density of ~3×10^6 viable cells/mL in the Expi293F™ expression medium. Plasmid DNA and ExpiFectamine™ 293 reagent were diluted with Opti-MEM™ I reduced serum media and incubated at room temperature for 5 min. After 15-20 min, ExpiFectamine™ 293/Plasmid DNA complexes were slowly added to Expi293F™ cells. Eighteen hours post-transfection, ExpiFectamine™ 293 Transfection Enhancer 1 and 2 were added to the transfected cells. Six days post-transfection, culture was harvested, and proteins were purified from culture supernatant by nickel affinity chromatography. The culture supernatant was incubated with Ni-Sepharose 6 Fast Flow resin (GE Healthcare) for 6-8 h at 4 °C. Non-specific proteins were removed by passing twenty-column volumes of wash buffer (PBS containing 25 mM Imidazole, pH 7.4). Bound proteins were eluted from the Ni-NTA column using 500 mM imidazole in PBS buffer, pH 7.4, and were dialyzed against PBS buffer using a 10 kDa (MWCO) dialysis membrane. The purity of purified protein samples was analyzed on SDS-PAGE.

Size Exclusion Chromatography-Multi Angle Light Scattering (SEC-MALS)

A Superdex-200 10/300 analytical column, equilibrated with PBS buffer, pH 7.4, was used for size exclusion chromatography-multi angle light scattering. 100 μg of purified protein samples were injected into the column, and protein peaks were resolved on a SHIMADZU HPLC at a flow rate

of 0.5 mL/min. Resolved peaks were subjected to In-line UV, refractive index, and triple-angle MALS scattering detectors. ASTRA™ software was used for acquired data analysis and molecular weight determination.

Differential Scanning Fluorimetry (nano-DSF)

A Prometheus NT.48 instrument was used to determine the thermal stability of the immunogens. The thermal unfolding of immunogens was monitored from 20 °C to 95 °C at a scan rate of 1 °C/min *(60)*.

Trypsin Proteolysis

The proteolytic stability of designed immunogens was studied by performing trypsin proteolysis. S2, RS2, and S2R were dialyzed against 50 mM Tris buffer (pH 7.5) containing 1 mM $CaCl_2$, followed by incubation with TPCK trypsin (protease) in a 1:50 molar ratio at 4 °C and 37 °C. At different time points, aliquots were taken out, and the reaction was quenched using 6X-SDS-loading dye. Collected samples were analyzed on 12 % SDS-PAGE.

Surface Plasmon Resonance (SPR)

The binding affinity of the S2, RS2, S2R and Spike immunogens to different RBD and S2-specific antibodies were measured using ProteOn XPR36 Protein Interaction Array V.3.1. The SPR sensor prism HC200M chip (Xantec bioanalytics) was first activated with EDC and sulfo-NHS. Then Protein G (10 µg/mL) was immobilized in the presence of 10 mM sodium acetate buffer, pH 4.0. Finally, excess sulfo-NHS esters were quenched using 1 M ethanolamine. 500 response units (R.U.) of ACE2-hFc, RBD specific monoclonal antibodies: CR3022, S309, ADG-2, H014, and S2-specific monoclonal antibodies: B6 and CC40.8 were immobilized. Different protein sample concentrations (100 nM, 50 nM, 25 nM, 12.5 nM, and 6.25 nM) were passed over the HC200M chip surface at a flow rate of 30 µL/min, followed by dissociation with PBS buffer containing 0.05% tween-20 (PBST). After each kinetic-binding assay, the chip was regenerated using 0.1 M Glycine-HCl, pH 2.7. Proteon Manager was used for fitting data to a simple 1:1 Langmuir interaction model to obtain kinetic parameters.

Formulation preparation with SWE adjuvant

The adjuvant SWE (squalene-in-water emulsion) was co-developed by the Vaccine Formulation Institute (Switzerland) and Seppic (France) and is available at GMP grade (Sepivac SWE™) under an open access model. Immunogens (S2, S2R or RS2) were formulated with SWE at 1:1 volume ratio. The formulation RS2 in combination with SWE was evaluated for 1 month stability

measuring adjuvant physicochemical characteristics and antigen integrity. Measurements included: visual inspection, particle size and polydispersity (DLS), zeta potential (ELS), pH, osmolality, and squalene content (HPLC). Antigen integrity was evaluated by ELISA.

Immunization Studies

(BALB/c mice immunizations): Groups of 6-8 weeks old, female BALB/c mice (n=5) were intramuscularly immunized with either 2 µg or 20 µg dose of SWE adjuvant formulated RS2 immunogen.

(hACE-2 expressing C57BL/6 transgenic mice immunizations): Groups of hACE-2 expressing transgenic mice (n=6/7) were intramuscularly immunized with 2 µg and/or 20 µg dose of SWE adjuvant formulated immunogens (S2, RS2, S2R, Spike, and RBD). B6N; DBA2-Tg(K18-hACE2)3068Mgef/Blisc (acrc:21000509) mice strain was generated and provided by the Mouse Genome Engineering Facility, NCBS Bangalore using the K18-hACE2 transgene plasmid, kindly donated by Dr Paul B. McCray *(61)*

(Syrian Hamster Immunizations): Groups of five female golden Syrian hamsters were intramuscularly immunized with either a 5 µg or 20 µg dose of SWE adjuvant-formulated immunogens (RS2, Spike, and RBD).

SWE adjuvant-treated animals were used as control. The sera samples from immunized and unimmunized animals were collected before prime (Day -1), 2 weeks post-prime (Day 14), and 14 days post-boost (Day 35) for endpoint ELISA and measuring neutralizing antibody titers. *Challenge Studies:* Twenty-one days following boost immunizations, immunized animals were intranasally challenged with either 10^5 pfu MA10, 10^5 pfu/ 10^4 pfu Beta, or 10^4 pfu Delta VOCs. The unimmunized challenged animals were used as control. Weight change of immunized-challenged animals, unimmunized-unchallenged animals (UC), and unimmunized-challenged control groups (VC) were monitored and recorded for 5-9 days. Post-challenge, lungs were harvested for viral titer estimation and histopathological examination as previously described *(23)*. For lung tissue histopathology scoring, we developed a scientific method using Mitchison's virulence scoring system with some modifications, considering the consolidation of lungs, severity of bronchial and alveolar inflammation, immune cell influx, and alveolar and perivascular edema *(23, 62)*. The histopathology scores were graded as 0-4 (4: Severe pathology; 3: Moderate pathology; 2: mild pathology; 1: Minor/minimum pathology; 0: No pathology).

ELISA- Endpoint titers of serum-binding antibodies

As described previously, endpoint titers of serum-binding antibodies were determined using ELISA *(24)*. Briefly, 96 well ELISA plates were coated with 4 μg/mL RBD (332-532 a.a) or Spike (1-1208 a.a) and incubated at 25 °C for 2-3 h. Plates were washed with PBST, followed by incubation and with blocking with 3 % skimmed milk (in PBST) at 25 °C for 1 h. Four-fold serially diluted antisera raised against immunogens were added to wells and incubated at 25 °C for 1 h. Following three washes with PBST, plates were incubated with 1:5000 diluted goat ALP-conjugated anti-mouse IgG secondary antibody at 25 °C for 1 h. Plates were washed thrice with PBST and incubated with pNPP liquid substrate at 37 °C for 30 min. Optical density (O.D.) was measured at 405 nm. The ELISA endpoint titers were determined as the highest sera dilution with an O.D. signal above 0.2 at 405 nm.

Pseudoviral neutralization assay

Psuedoviral neutralization assays were performed as previously described *(23)*. The genes encoding Spike proteins from VOC were synthesized at GenScript (USA). Pseudovirus neutralization titers (ID_{50}) were defined as the serum dilution at which the infectivity of the virus is reduced to 50%.

Statistical Analysis:

Data analysis was performed using GraphPad Prism software 9.0.0. The ELISA binding, neutralization titers, and pseudoviral virus neutralization titer data were analyzed with a two-tailed Mann–Whitney test and non-parametric Kruskal–Wallis with Dunn's multiple, respectively. Weight changes in mice and hamsters were analyzed with a two-tailed Student's t-test. (* indicates $p < 0.05$, ** indicates $p < 0.01$, *** indicates $p < 0.001$, **** indicates $p < 0.0001$).

All mice and Hamster immunization studies were approved by the Institutional Animal Ethics Committee (CAF/ETHICS/847/2021; CAF/ETHICS/887/2022). These were carried out at the Central Animal Facility (CAF), Indian Institute of Science, according to CPCSEA and ARRIVE guidelines.

References

1. Q. Li, X. Guan, P. Wu, X. Wang, L. Zhou, Y. Tong, R. Ren, K. S. M. Leung, E. H. Y. Lau, J. Y. Wong, X. Xing, N. Xiang, Y. Wu, C. Li, Q. Chen, D. Li, T. Liu, J. Zhao, M. Liu, W. Tu, C. Chen, L. Jin, R. Yang, Q. Wang, S. Zhou, R. Wang, H. Liu, Y. Luo, Y. Liu, G. Shao, H. Li, Z. Tao, Y. Yang, Z. Deng, B. Liu, Z. Ma, Y. Zhang, G. Shi, T. T. Y. Lam, J. T. Wu, G. F. Gao, B. J. Cowling, B. Yang, G. M. Leung, Z. Feng, Early Transmission Dynamics in Wuhan, China, of Novel Coronavirus–Infected Pneumonia. *New England Journal of Medicine* **382**, 1199–1207 (2020).
2. S. Xia, K. Duan, Y. Zhang, D. Zhao, H. Zhang, Z. Xie, X. Li, C. Peng, Y. Zhang, W. Zhang, Y. Yang, W. Chen, X. Gao, W. You, X. Wang, Z. Wang, Z. Shi, Y. Wang, X. Yang, L. Zhang, L. Huang, Q. Wang, J. Lu, Y. Yang, J. Guo, W. Zhou, X. Wan, C. Wu, W. Wang, S. Huang, J. Du, Z. Meng, A. Pan, Z. Yuan, S. Shen, W. Guo, X. Yang, Effect of an Inactivated Vaccine Against SARS-CoV-2 on Safety and Immunogenicity Outcomes: Interim Analysis of 2 Randomized Clinical Trials. *JAMA* **324**, 951–960 (2020).
3. L. A. Jackson, E. J. Anderson, N. G. Rouphael, P. C. Roberts, M. Makhene, R. N. Coler, M. P. McCullough, J. D. Chappell, M. R. Denison, L. J. Stevens, A. J. Pruijssers, A. McDermott, B. Flach, N. A. Doria-Rose, K. S. Corbett, K. M. Morabito, S. O'Dell, S. D. Schmidt, P. A. Swanson, M. Padilla, J. R. Mascola, K. M. Neuzil, H. Bennett, W. Sun, E. Peters, M. Makowski, J. Albert, K. Cross, W. Buchanan, R. Pikaart-Tautges, J. E. Ledgerwood, B. S. Graham, J. H. Beigel, An mRNA Vaccine against SARS-CoV-2 — Preliminary Report. *New England Journal of Medicine* **383**, 1920–1931 (2020).
4. C. Keech, G. Albert, I. Cho, A. Robertson, P. Reed, S. Neal, J. S. Plested, M. Zhu, S. Cloney-Clark, H. Zhou, G. Smith, N. Patel, M. B. Frieman, R. E. Haupt, J. Logue, M. McGrath, S. Weston, P. A. Piedra, C. Desai, K. Callahan, M. Lewis, P. Price-Abbott, N. Formica, V. Shinde, L. Fries, J. D. Lickliter, P. Griffin, B. Wilkinson, G. M. Glenn, Phase 1–2 Trial of a SARS-CoV-2 Recombinant Spike Protein Nanoparticle Vaccine. *New England Journal of Medicine* **383**, 2320–2332 (2020).
5. P. M. Folegatti, K. J. Ewer, P. K. Aley, B. Angus, S. Becker, S. Belij-Rammerstorfer, D. Bellamy, S. Bibi, M. Bittaye, E. A. Clutterbuck, C. Dold, S. N. Faust, A. Finn, A. L. Flaxman, B. Hallis, P. Heath, D. Jenkin, R. Lazarus, R. Makinson, A. M. Minassian, K. M. Pollock, M. Ramasamy, H. Robinson, M. Snape, R. Tarrant, M. Voysey, C. Green, A. D. Douglas, A. V. S. Hill, T. Lambe, S. C. Gilbert, A. J. Pollard, J. Aboagye, K. Adams, A. Ali, E. Allen, J. L. Allison, R. Anslow, E. H. Arbe-Barnes, G. Babbage, K. Baillie, M. Baker, N. Baker, P. Baker, I. Baleanu, J. Ballaminut, E. Barnes, J. Barrett, L. Bates, A. Batten, K. Beadon, R. Beckley, E. Berrie, L. Berry, A. Beveridge, K. R. Bewley, E. M. Bijker, T. Bingham, L. Blackwell, C. L. Blundell, E. Bolam, E. Boland, N. Borthwick, T. Bower, A. Boyd, T. Brenner, P. D. Bright, C. Brown-O'Sullivan, E. Brunt, J. Burbage, S. Burge, K. R. Buttigieg, N. Byard, I. Cabera Puig, A. Calvert, S. Camara, M. Cao, F. Cappuccini, M. Carr, M. W. Carroll, V. Carter, K. Cathie, R. J. Challis, S. Charlton, I. Chelysheva, J. S. Cho, P. Cicconi, L. Cifuentes, H. Clark, E. Clark, T. Cole, R. Colin-Jones, C. P. Conlon, A. Cook, N. S. Coombes, R. Cooper, C. A. Cosgrove, K. Coy, W. E. M. Crocker, C. J. Cunningham, B. E. Damratoski, L. Dando, M. S. Datoo, H. Davies, H. de Graaf, T. Demissie, C. di Maso, I. Dietrich, T. Dong, F. R. Donnellan, N. Douglas, C. Downing, J. Drake, R. Drake-Brockman, R. E. Drury, S. J. Dunachie, N. J. Edwards, F. D. L. Edwards, C. J. Edwards, S. C. Elias, M. J. Elmore, K. R. W. Emary, M. R. English, S. Fagerbrink, S. Felle, S. Feng, S. Field, C. Fixmer, C. Fletcher, K. J. Ford, J. Fowler, P. Fox, E. Francis, J. Frater, J. Furze, M.

Fuskova, E. Galiza, D. Gbesemete, C. Gilbride, K. Godwin, G. Gorini, L. Goulston, C. Grabau, L. Gracie, Z. Gray, L. B. Guthrie, M. Hackett, S. Halwe, E. Hamilton, J. Hamlyn, B. Hanumunthadu, I. Harding, S. A. Harris, A. Harris, D. Harrison, C. Harrison, T. C. Hart, L. Haskell, S. Hawkins, I. Head, J. A. Henry, J. Hill, S. H. C. Hodgson, M. M. Hou, E. Howe, N. Howell, C. Hutlin, S. Ikram, C. Isitt, P. Iveson, S. Jackson, F. Jackson, S. W. James, M. Jenkins, E. Jones, K. Jones, C. E. Jones, B. Jones, R. Kailath, K. Karampatsas, J. Keen, S. Kelly, D. Kelly, D. Kerr, S. Kerridge, L. Khan, U. Khan, A. Killen, J. Kinch, T. B. King, L. King, J. King, L. Kingham-Page, P. Klenerman, F. Knapper, J. C. Knight, D. Knott, S. Koleva, A. Kupke, C. W. Larkworthy, J. P. J. Larwood, A. Laskey, A. M. Lawrie, A. Lee, K. Y. Ngan Lee, E. A. Lees, H. Legge, A. Lelliott, N. M. Lemm, A. M. Lias, A. Linder, S. Lipworth, X. Liu, S. Liu, R. Lopez Ramon, M. Lwin, F. Mabesa, M. Madhavan, G. Mallett, K. Mansatta, I. Marcal, S. Marinou, E. Marlow, J. L. Marshall, J. Martin, J. McEwan, L. McInroy, G. Meddaugh, A. J. Mentzer, N. Mirtorabi, M. Moore, E. Moran, E. Morey, V. Morgan, S. J. Morris, H. Morrison, G. Morshead, R. Morter, Y. F. Mujadidi, J. Muller, T. Munera-Huertas, C. Munro, A. Munro, S. Murphy, V. J. Munster, P. Mweu, A. Noé, F. L. Nugent, E. Nuthall, K. O'Brien, D. O'Connor, B. Oguti, J. L. Oliver, C. Oliveira, P. J. O'Reilly, M. Osborn, P. Osborne, C. Owen, D. Owens, N. Owino, M. Pacurar, K. Parker, H. Parracho, M. Patrick-Smith, V. Payne, J. Pearce, Y. Peng, M. P. Peralta Alvarez, J. Perring, K. Pfafferott, D. Pipini, E. Plested, H. Pluess-Hall, K. Pollock, I. Poulton, L. Presland, S. Provstgaard-Morys, D. Pulido, K. Radia, F. Ramos Lopez, J. Rand, H. Ratcliffe, T. Rawlinson, S. Rhead, A. Riddell, A. J. Ritchie, H. Roberts, J. Robson, S. Roche, C. Rohde, C. S. Rollier, R. Romani, I. Rudiansyah, S. Saich, S. Sajjad, S. Salvador, L. Sanchez Riera, H. Sanders, K. Sanders, S. Sapaun, C. Sayce, E. Schofield, G. Screaton, B. Selby, C. Semple, H. R. Sharpe, I. Shaik, A. Shea, H. Shelton, S. Silk, L. Silva-Reyes, D. T. Skelly, H. Smee, C. C. Smith, D. J. Smith, R. Song, A. J. Spencer, E. Stafford, A. Steele, E. Stefanova, L. Stockdale, A. Szigeti, A. Tahiri-Alaoui, M. Tait, H. Talbot, R. Tanner, I. J. Taylor, V. Taylor, R. te Water Naude, N. Thakur, Y. Themistocleous, A. Themistocleous, M. Thomas, T. M. Thomas, A. Thompson, S. Thomson-Hill, J. Tomlins, S. Tonks, J. Towner, N. Tran, J. A. Tree, A. Truby, K. Turkentine, C. Turner, N. Turner, S. Turner, T. Tuthill, M. Ulaszewska, R. Varughese, N. van Doremalen, K. Veighey, M. K. Verheul, I. Vichos, E. Vitale, L. Walker, M. E. E. Watson, B. Welham, J. Wheat, C. White, R. White, A. T. Worth, D. Wright, S. Wright, X. L. Yao, Y. Yau, Safety and immunogenicity of the ChAdOx1 nCoV-19 vaccine against SARS-CoV-2: a preliminary report of a phase 1/2, single-blind, randomised controlled trial. *The Lancet* **396**, 467–478 (2020).

6. D. Y. Logunov, I. v. Dolzhikova, O. v. Zubkova, A. I. Tukhvatullin, D. v. Shcheblyakov, A. S. Dzharullaeva, D. M. Grousova, A. S. Erokhova, A. v. Kovyrshina, A. G. Botikov, F. M. Izhaeva, O. Popova, T. A. Ozharovskaya, I. B. Esmagambetov, I. A. Favorskaya, D. I. Zrelkin, D. v. Voronina, D. N. Shcherbinin, A. S. Semikhin, Y. v. Simakova, E. A. Tokarskaya, N. L. Lubenets, D. A. Egorova, M. M. Shmarov, N. A. Nikitenko, L. F. Morozova, E. A. Smolyarchuk, E. v. Kryukov, V. F. Babira, S. v. Borisevich, B. S. Naroditsky, A. L. Gintsburg, Safety and immunogenicity of an rAd26 and rAd5 vector-based heterologous prime-boost COVID-19 vaccine in two formulations: two open, non-randomised phase 1/2 studies from Russia. *Lancet* **396**, 887–897 (2020).

7. Y. Zhang, G. Zeng, H. Pan, C. Li, Y. Hu, K. Chu, W. Han, Z. Chen, R. Tang, W. Yin, X. Chen, Y. Hu, X. Liu, C. Jiang, J. Li, M. Yang, Y. Song, X. Wang, Q. Gao, F. Zhu, Safety, tolerability, and immunogenicity of an inactivated SARS-CoV-2 vaccine in healthy adults aged 18–59 years: a randomised, double-blind, placebo-controlled, phase 1/2 clinical trial. *Lancet Infect Dis* **21**, 181–192 (2021).

8. F. C. Zhu, Y. H. Li, X. H. Guan, L. H. Hou, W. J. Wang, J. X. Li, S. P. Wu, B. sen Wang, Z. Wang, L. Wang, S. Y. Jia, H. D. Jiang, L. Wang, T. Jiang, Y. Hu, J. B. Gou, S. B. Xu, J. J. Xu, X. W. Wang, W. Wang, W. Chen, Safety, tolerability, and immunogenicity of a recombinant adenovirus type-5 vectored COVID-19 vaccine: a dose-escalation, open-label, non-randomised, first-in-human trial. *The Lancet* **395**, 1845–1854 (2020).
9. E. E. Walsh, R. W. Frenck, A. R. Falsey, N. Kitchin, J. Absalon, A. Gurtman, S. Lockhart, K. Neuzil, M. J. Mulligan, R. Bailey, K. A. Swanson, P. Li, K. Koury, W. Kalina, D. Cooper, C. Fontes-Garfias, P.-Y. Shi, Ö. Türeci, K. R. Tompkins, K. E. Lyke, V. Raabe, P. R. Dormitzer, K. U. Jansen, U. Şahin, W. C. Gruber, Safety and Immunogenicity of Two RNA-Based Covid-19 Vaccine Candidates. *New England Journal of Medicine* **383**, 2439–2450 (2020).
10. B. Ganneru, H. Jogdand, V. K. Dharam, N. R. Molugu, S. D. Prasad, S. Vellimudu, K. M. Ella, R. Ravikrishnan, A. Awasthi, J. Jose, P. Rao, D. Kumar, R. Ella, P. Abraham, P. Yadav, G. N. Sapkal, A. Shete, G. R. Desphande, S. Mohandas, A. Basu, N. Gupta, K. M. Vadrevu, Evaluation of Safety and Immunogenicity of an Adjuvanted, TH-1 Skewed, Whole Virion InactivatedSARS-CoV-2 Vaccine - BBV152. *bioRxiv* , 2020.09.09.285445 (2020).
11. A. C. Walls, Y. J. Park, M. A. Tortorici, A. Wall, A. T. McGuire, D. Veesler, Structure, Function, and Antigenicity of the SARS-CoV-2 Spike Glycoprotein. *Cell* **181**, 281-292.e6 (2020).
12. J. Shang, Y. Wan, C. Luo, G. Ye, Q. Geng, A. Auerbach, F. Li, Cell entry mechanisms of SARS-CoV-2. *Proc Natl Acad Sci U S A* **117**, 11727–11734 (2020).
13. Q. Wang, Y. Zhang, L. Wu, S. Niu, C. Song, Z. Zhang, G. Lu, C. Qiao, Y. Hu, K. Y. Yuen, Q. Wang, H. Zhou, J. Yan, J. Qi, Structural and Functional Basis of SARS-CoV-2 Entry by Using Human ACE2. *Cell* **181**, 894-904.e9 (2020).
14. C. O. Barnes, C. A. Jette, M. E. Abernathy, K. M. A. Dam, S. R. Esswein, H. B. Gristick, A. G. Malyutin, N. G. Sharaf, K. E. Huey-Tubman, Y. E. Lee, D. F. Robbiani, M. C. Nussenzweig, A. P. West, P. J. Bjorkman, SARS-CoV-2 neutralizing antibody structures inform therapeutic strategies. *Nature* **588**, 682–687 (2020).
15. Y. Wu, F. Wang, C. Shen, W. Peng, D. Li, C. Zhao, Z. Li, S. Li, Y. Bi, Y. Yang, Y. Gong, H. Xiao, Z. Fan, S. Tan, G. Wu, W. Tan, X. Lu, C. Fan, Q. Wang, Y. Liu, C. Zhang, J. Qi, G. F. Gao, F. Gao, L. Liu, A noncompeting pair of human neutralizing antibodies block COVID-19 virus binding to its receptor ACE2. *Science (1979)* **368**, 1274–1278 (2020).
16. J. Huo, Y. Zhao, J. Ren, D. Zhou, H. M. E. Duyvesteyn, H. M. Ginn, L. Carrique, T. Malinauskas, R. R. Ruza, P. N. M. Shah, T. K. Tan, P. Rijal, N. Coombes, K. R. Bewley, J. A. Tree, J. Radecke, N. G. Paterson, P. Supasa, J. Mongkolsapaya, G. R. Screaton, M. Carroll, A. Townsend, E. E. Fry, R. J. Owens, D. I. Stuart, Neutralization of SARS-CoV-2 by Destruction of the Prefusion Spike. *Cell Host Microbe* **28**, 445-454.e6 (2020).
17. D. Pinto, Y. J. Park, M. Beltramello, A. C. Walls, M. A. Tortorici, S. Bianchi, S. Jaconi, K. Culap, F. Zatta, A. de Marco, A. Peter, B. Guarino, R. Spreafico, E. Cameroni, J. B. Case, R. E. Chen, C. Havenar-Daughton, G. Snell, A. Telenti, H. W. Virgin, A. Lanzavecchia, M. S. Diamond, K. Fink, D. Veesler, D. Corti, Cross-neutralization of SARS-CoV-2 by a human monoclonal SARS-CoV antibody. *Nature* **583**, 290–295 (2020).
18. P. J. M. Brouwer, T. G. Caniels, K. van der Straten, J. L. Snitselaar, Y. Aldon, S. Bangaru, J. L. Torres, N. M. A. Okba, M. Claireaux, G. Kerster, A. E. H. Bentlage, M. M. van Haaren, D. Guerra, J. A. Burger, E. E. Schermer, K. D. Verheul, N. van der Velde, A. van der Kooi, J. van Schooten, M. J. van Breemen, T. P. L. Bijl, K. Sliepen, A. Aartse, R. Derking, I. Bontjer, N. A. Kootstra, W. Joost Wiersinga, G. Vidarsson, B. L. Haagmans, A. B. Ward, G. J. de Bree, R. W.

Sanders, M. J. van Gils, Potent neutralizing antibodies from COVID-19 patients define multiple targets of vulnerability. *Science (1979)* **369**, 643–650 (2020).
19. C. Wang, R. van Haperen, J. Gutiérrez-Álvarez, W. Li, N. M. A. Okba, I. Albulescu, I. Widjaja, B. van Dieren, R. Fernandez-Delgado, I. Sola, D. L. Hurdiss, O. Daramola, F. Grosveld, F. J. M. van Kuppeveld, B. L. Haagmans, L. Enjuanes, D. Drabek, B. J. Bosch, A conserved immunogenic and vulnerable site on the coronavirus spike protein delineated by cross-reactive monoclonal antibodies. *Nat Commun* **12**, 1–15 (2021).
20. T. F. Rogers, F. Zhao, D. Huang, N. Beutler, A. Burns, W. T. He, O. Limbo, C. Smith, G. Song, J. Woehl, L. Yang, R. K. Abbott, S. Callaghan, E. Garcia, J. Hurtado, M. Parren, L. Peng, S. Ramirez, J. Ricketts, M. J. Ricciardi, S. A. Rawlings, N. C. Wu, M. Yuan, D. M. Smith, D. Nemazee, J. R. Teijaro, J. E. Voss, I. A. Wilson, R. Andrabi, B. Briney, E. Landais, D. Sok, J. G. Jardine, D. R. Burton, Isolation of potent SARS-CoV-2 neutralizing antibodies and protection from disease in a small animal model. *Science (1979)* **369**, 956–963 (2020).
21. S. Thuluva, V. Paradkar, S. R. Gunneri, V. Yerroju, R. Mogulla, K. Turaga, M. Kyasani, S. K. Manoharan, G. Medigeshi, J. Singh, H. Shaman, C. Singh, V. Rao A, Evaluation of safety and immunogenicity of receptor-binding domain-based COVID-19 vaccine (Corbevax) to select the optimum formulation in open-label, multicentre, and randomised phase-1/2 and phase-2 clinical trials. *EBioMedicine* **83**, 104217 (2022).
22. S. K. Malladi, R. Singh, S. Pandey, S. Gayathri, K. Kanjo, S. Ahmed, M. S. Khan, P. Kalita, N. Girish, A. Upadhyaya, P. Reddy, I. Pramanick, M. Bhasin, S. Mani, S. Bhattacharyya, J. Joseph, K. Thankamani, V. S. Raj, S. Dutta, R. Singh, G. Nadig, R. Varadarajan, Design of a highly thermotolerant, immunogenic SARS-CoV-2 spike fragment. *Journal of Biological Chemistry* **296**, 100025 (2021).
23. S. K. Malladi, U. R. Patel, R. S. Rajmani, R. Singh, S. Pandey, S. Kumar, S. Khaleeq, P. J. van Vuren, S. Riddell, S. Goldie, S. Gayathri, D. Chakraborty, P. Kalita, I. Pramanick, N. Agarwal, P. Reddy, N. Girish, A. Upadhyaya, M. S. Khan, K. Kanjo, M. Bhat, S. Mani, S. Bhattacharyya, S. Siddiqui, A. Tyagi, S. Jha, R. Pandey, S. Tripathi, S. Dutta, A. J. McAuley, N. B. Singanallur, S. S. Vasan, R. P. Ringe, R. Varadarajan, Immunogenicity and Protective Efficacy of a Highly Thermotolerant, Trimeric SARS-CoV-2 Receptor Binding Domain Derivative. *ACS Infect Dis* **7**, 2546–2564 (2021).
24. S. Ahmed, M. S. Khan, S. Gayathri, R. Singh, S. Kumar, U. R. Patel, S. K. Malladi, R. S. Rajmani, P. J. van Vuren, S. Riddell, S. Goldie, N. Girish, P. Reddy, A. Upadhyaya, S. Pandey, S. Siddiqui, A. Tyagi, S. Jha, R. Pandey, O. Khatun, R. Narayan, S. Tripathi, A. J. McAuley, N. B. Singanallur, S. S. Vasan, R. P. Ringe, R. Varadarajan, A Stabilized, Monomeric, Receptor Binding Domain Elicits High-Titer Neutralizing Antibodies Against All SARS-CoV-2 Variants of Concern. *Front Immunol* **12**, 5214 (2021).
25. W. T. Harvey, A. M. Carabelli, B. Jackson, R. K. Gupta, E. C. Thomson, E. M. Harrison, C. Ludden, R. Reeve, A. Rambaut, S. J. Peacock, D. L. Robertson, SARS-CoV-2 variants, spike mutations and immune escape. *Nature Reviews Microbiology 2021 19:7* **19**, 409–424 (2021).
26. K. T. Ng, N. K. Mohd-Ismail, Y. J. Tan, Spike S2 Subunit: The Dark Horse in the Race for Prophylactic and Therapeutic Interventions against SARS-CoV-2. *Vaccines 2021, Vol. 9, Page 178* **9**, 178 (2021).
27. M. M. Sauer, M. A. Tortorici, Y. J. Park, A. C. Walls, L. Homad, O. J. Acton, J. E. Bowen, C. Wang, X. Xiong, W. de van der Schueren, J. Quispe, B. G. Hoffstrom, B. J. Bosch, A. T. McGuire, D. Veesler, Structural basis for broad coronavirus neutralization. *Nat Struct Mol Biol* , 1–9 (2021).

28. A. Z. Wec, D. Wrapp, A. S. Herbert, D. P. Maurer, D. Haslwanter, M. Sakharkar, R. K. Jangra, M. Eugenia Dieterle, A. Lilov, D. Huang, L. v. Tse, N. v. Johnson, C. L. Hsieh, N. Wang, J. H. Nett, E. Champney, I. Burnina, M. Brown, S. Lin, M. Sinclair, C. Johnson, S. Pudi, R. Bortz, A. S. Wirchnianski, E. Laudermilch, C. Florez, J. Maximilian Fels, C. M. O'Brien, B. S. Graham, D. Nemazee, D. R. Burton, R. S. Baric, J. E. Voss, K. Chandran, J. M. Dye, J. S. McLellan, L. M. Walker, Broad neutralization of SARS-related viruses by human monoclonal antibodies. *Science (1979)* **369**, 731–736 (2020).
29. G. Song, W. He, S. Callaghan, F. Anzanello, D. Huang, J. Ricketts, J. L. Torres, N. Beutler, L. Peng, S. Vargas, J. Cassell, M. Parren, L. Yang, C. Ignacio, D. M. Smith, J. E. Voss, D. Nemazee, A. B. Ward, T. Rogers, D. R. Burton, R. Andrabi, Cross-reactive serum and memory B-cell responses to spike protein in SARS-CoV-2 and endemic coronavirus infection. *Nat Commun* **12**, 2938 (2021).
30. W. Li, Y. Chen, J. Prévost, I. Ullah, M. Lu, S. Y. Gong, A. Tauzin, R. Gasser, D. Vézina, S. P. Anand, G. Goyette, D. Chaterjee, S. Ding, W. D. Tolbert, M. W. Grunst, Y. Bo, S. Zhang, J. Richard, F. Zhou, R. K. Huang, L. Esser, A. Zeher, M. Côté, P. Kumar, J. Sodroski, D. Xia, P. D. Uchil, M. Pazgier, A. Finzi, W. Mothes, Structural basis and mode of action for two broadly neutralizing antibodies against SARS-CoV-2 emerging variants of concern. *Cell Rep* **38**, 110210 (2022).
31. C. L. Hsieh, A. P. Werner, S. R. Leist, L. J. Stevens, E. Falconer, J. A. Goldsmith, C. W. Chou, O. M. Abiona, A. West, K. Westendorf, K. Muthuraman, E. J. Fritch, K. H. Dinnon, A. Schäfer, M. R. Denison, J. D. Chappell, R. S. Baric, B. S. Graham, K. S. Corbett, J. S. McLellan, Stabilized coronavirus spike stem elicits a broadly protective antibody. *Cell Rep* **37**, 109929 (2021).
32. P. Zhou, M. Yuan, G. Song, N. Beutler, N. Shaabani, D. Huang, W. T. He, X. Zhu, S. Callaghan, P. Yong, F. Anzanello, L. Peng, J. Ricketts, M. Parren, E. Garcia, S. A. Rawlings, D. M. Smith, D. Nemazee, J. R. Teijaro, T. F. Rogers, I. A. Wilson, D. R. Burton, R. Andrabi, A human antibody reveals a conserved site on beta-coronavirus spike proteins and confers protection against SARS-CoV-2 infection. *Sci Transl Med* **14** (2022).
33. N. K. Hurlburt, L. J. Homad, I. Sinha, M. F. Jennewein, A. J. MacCamy, Y. H. Wan, J. Boonyaratanakornkit, A. M. Sholukh, A. M. Jackson, P. Zhou, D. R. Burton, R. Andrabi, G. Ozorowski, A. B. Ward, L. Stamatatos, M. Pancera, A. T. McGuire, Structural definition of a pan-sarbecovirus neutralizing epitope on the spike S2 subunit. *Communications Biology 2022 5:1* **5**, 1–13 (2022).
34. D. Pinto, M. M. Sauer, N. Czudnochowski, J. S. Low, M. Alejandra Tortorici, M. P. Housley, J. Noack, A. C. Walls, J. E. Bowen, B. Guarino, L. E. Rosen, J. di Iulio, J. Jerak, H. Kaiser, S. Islam, S. Jaconi, N. Sprugasci, K. Culap, R. Abdelnabi, C. Foo, L. Coelmont, I. Bartha, S. Bianchi, C. Silacci-Fregni, J. Bassi, R. Marzi, E. Vetti, A. Cassotta, A. Ceschi, P. Ferrari, P. E. Cippà, O. Giannini, S. Ceruti, C. Garzoni, A. Riva, F. Benigni, E. Cameroni, L. Piccoli, M. S. Pizzuto, M. Smithey, D. Hong, A. Telenti, F. A. Lempp, J. Neyts, C. Havenar-Daughton, A. Lanzavecchia, F. Sallusto, G. Snell, H. W. Virgin, M. Beltramello, D. Corti, D. Veesler, Broad betacoronavirus neutralization by a stem helix–specific human antibody. *Science (1979)* **373**, 1109–1116 (2021).
35. Y. Huang, A. W. Nguyen, C.-L. Hsieh, R. Silva, O. S. Olaluwoye, R. E. Wilen, T. S. Kaoud, L. R. Azouz, A. N. Qerqez, K. C. Le, A. L. Bohanon, A. M. DiVenere, Y. Liu, A. G. Lee, D. Amengor, S. R. Shoemaker, S. M. Costello, S. Marqusee, K. N. Dalby, S. D'Arcy, J. S. McLellan, J. A. Maynard, Identification of a conserved neutralizing epitope present on spike proteins from all highly pathogenic coronaviruses. *bioRxiv* , 2021.01.31.428824 (2021).

36. M. F. Jennewein, A. J. MacCamy, N. R. Akins, J. Feng, L. J. Homad, N. K. Hurlburt, E. Seydoux, Y. H. Wan, A. B. Stuart, V. V. Edara, K. Floyd, A. Vanderheiden, J. R. Mascola, N. Doria-Rose, L. Wang, E. S. Yang, H. Y. Chu, J. L. Torres, G. Ozorowski, A. B. Ward, R. E. Whaley, K. W. Cohen, M. Pancera, M. J. McElrath, J. A. Englund, A. Finzi, M. S. Suthar, A. T. McGuire, L. Stamatatos, Isolation and characterization of cross-neutralizing coronavirus antibodies from COVID-19+ subjects. *Cell Rep* **36**, 109353 (2021).
37. S. Iketani, L. Liu, Y. Guo, L. Liu, J. F. W. Chan, Y. Huang, M. Wang, Y. Luo, J. Yu, H. Chu, K. K. H. Chik, T. T. T. Yuen, M. T. Yin, M. E. Sobieszczyk, Y. Huang, K. Y. Yuen, H. H. Wang, Z. Sheng, D. D. Ho, Antibody evasion properties of SARS-CoV-2 Omicron sublineages. *Nature* **604**, 553–556 (2022).
38. L. Liu, S. Iketani, Y. Guo, J. F. W. Chan, M. Wang, L. Liu, Y. Luo, H. Chu, Y. Huang, M. S. Nair, J. Yu, K. K. H. Chik, T. T. T. Yuen, C. Yoon, K. K. W. To, H. Chen, M. T. Yin, M. E. Sobieszczyk, Y. Huang, H. H. Wang, Z. Sheng, K. Y. Yuen, D. D. Ho, Striking antibody evasion manifested by the Omicron variant of SARS-CoV-2. *Nature* **602**, 676–681 (2022).
39. P. Wang, M. S. Nair, L. Liu, S. Iketani, Y. Luo, Y. Guo, M. Wang, J. Yu, B. Zhang, P. D. Kwong, B. S. Graham, J. R. Mascola, J. Y. Chang, M. T. Yin, M. Sobieszczyk, C. A. Kyratsous, L. Shapiro, Z. Sheng, Y. Huang, D. D. Ho, Antibody resistance of SARS-CoV-2 variants B.1.351 and B.1.1.7. *Nature 2021 593:7857* **593**, 130–135 (2021).
40. W. N. Voss, Y. J. Hou, N. v. Johnson, G. Delidakis, J. E. Kim, K. Javanmardi, A. P. Horton, F. Bartzoka, C. J. Paresi, Y. Tanno, C. W. Chou, S. A. Abbasi, W. Pickens, K. George, D. R. Boutz, D. M. Towers, J. R. McDaniel, D. Billick, J. Goike, L. Rowe, D. Batra, J. Pohl, J. Lee, S. Gangappa, S. Sambhara, M. Gadush, N. Wang, M. D. Person, B. L. Iverson, J. D. Gollihar, J. M. Dye, A. S. Herbert, I. J. Finkelstein, R. S. Baric, J. S. McLellan, G. Georgiou, J. J. Lavinder, G. C. Ippolito, Prevalent, protective, and convergent IgG recognition of SARS-CoV-2 non-RBD spike epitopes. *Science* **372**, 1108–1112 (2021).
41. L. Du, Y. Yang, X. Zhang, Neutralizing antibodies for the prevention and treatment of COVID-19. *Cellular & Molecular Immunology 2021 18:10* **18**, 2293–2306 (2021).
42. G. Bommakanti, M. P. Citron, R. W. Hepler, C. Callahan, G. J. Heidecker, T. A. Najar, X. Lu, J. G. Joyce, J. W. Shiver, D. R. Casimiro, J. ter Meulen, X. Liang, R. Varadarajan, Design of an HA2-based escherichia coli expressed influenza immunogen that protects mice from pathogenic challenge. *Proc Natl Acad Sci U S A* **107**, 13701–13706 (2010).
43. V. V. A. Mallajosyula, M. Citron, F. Ferrara, X. Lu, C. Callahan, G. J. Heidecker, S. P. Sarma, J. A. Flynn, N. J. Temperton, X. Liang, R. Varadarajan, Influenza hemagglutinin stem-fragment immunogen elicits broadly neutralizing antibodies and confers heterologous protection. *Proc Natl Acad Sci U S A* **111**, E2514–E2523 (2014).
44. J. Pallesen, N. Wang, K. S. Corbett, D. Wrapp, R. N. Kirchdoerfer, H. L. Turner, C. A. Cottrell, M. M. Becker, L. Wang, W. Shi, W. P. Kong, E. L. Andres, A. N. Kettenbach, M. R. Denison, J. D. Chappell, B. S. Graham, A. B. Ward, J. S. McLellan, Immunogenicity and structures of a rationally designed prefusion MERS-CoV spike antigen. *Proc Natl Acad Sci U S A* **114**, E7348–E7357 (2017).
45. A. Krarup, D. Truan, P. Furmanova-Hollenstein, L. Bogaert, P. Bouchier, I. J. M. Bisschop, M. N. Widjojoatmodjo, R. Zahn, H. Schuitemaker, J. S. McLellan, J. P. M. Langedijk, A highly stable prefusion RSV F vaccine derived from structural analysis of the fusion mechanism. *Nature Communications 2015 6:1* **6**, 1–12 (2015).
46. R. N. Kirchdoerfer, N. Wang, J. Pallesen, D. Wrapp, H. L. Turner, C. A. Cottrell, K. S. Corbett, B. S. Graham, J. S. McLellan, A. B. Ward, Stabilized coronavirus spikes are resistant to

conformational changes induced by receptor recognition or proteolysis. *Scientific Reports 2018 8:1* **8**, 1–11 (2018).
47. D. Wrapp, N. Wang, K. S. Corbett, J. A. Goldsmith, C.-L. Hsieh, O. Abiona, B. S. Graham, J. S. McLellan, Cryo-EM structure of the 2019-nCoV spike in the prefusion conformation. *Science (1979)* **367**, 1260–1263 (2020).
48. C. L. Hsieh, J. A. Goldsmith, J. M. Schaub, A. M. DiVenere, H. C. Kuo, K. Javanmardi, K. C. Le, D. Wrapp, A. G. Lee, Y. Liu, C. W. Chou, P. O. Byrne, C. K. Hjorth, N. v. Johnson, J. Ludes-Meyers, A. W. Nguyen, J. Park, N. Wang, D. Amengor, J. J. Lavinder, G. C. Ippolito, J. A. Maynard, I. J. Finkelstein, J. S. McLellan, Structure-based design of prefusion-stabilized SARS-CoV-2 spikes. *Science (1979)* **369**, 1501–1505 (2020).
49. A. C. Walls, M. C. Miranda, A. Schäfer, M. N. Pham, A. Greaney, P. S. Arunachalam, M. J. Navarro, M. A. Tortorici, K. Rogers, M. A. O'Connor, L. Shirreff, D. E. Ferrell, J. Bowen, N. Brunette, E. Kepl, S. K. Zepeda, T. Starr, C. L. Hsieh, B. Fiala, S. Wrenn, D. Pettie, C. Sydeman, K. R. Sprouse, M. Johnson, A. Blackstone, R. Ravichandran, C. Ogohara, L. Carter, S. W. Tilles, R. Rappuoli, S. R. Leist, D. R. Martinez, M. Clark, R. Tisch, D. T. O'Hagan, R. van der Most, W. C. van Voorhis, D. Corti, J. S. McLellan, H. Kleanthous, T. P. Sheahan, K. D. Smith, D. H. Fuller, F. Villinger, J. Bloom, B. Pulendran, R. S. Baric, N. P. King, D. Veesler, Elicitation of broadly protective sarbecovirus immunity by receptor-binding domain nanoparticle vaccines. *Cell* **184**, 5432-5447.e16 (2021).
50. A. A. Cohen, N. van Doremalen, A. J. Greaney, H. Andersen, A. Sharma, T. N. Starr, J. R. Keeffe, C. Fan, J. E. Schulz, P. N. P. Gnanapragasam, L. M. Kakutani, A. P. West, G. Saturday, Y. E. Lee, H. Gao, C. A. Jette, M. G. Lewis, T. K. Tan, A. R. Townsend, J. D. Bloom, V. J. Munster, P. J. Bjorkman, Mosaic RBD nanoparticles protect against challenge by diverse sarbecoviruses in animal models. *Science (1979)* **377** (2022).
51. A. A. Cohen, P. N. P. Gnanapragasam, Y. E. Lee, P. R. Hoffman, S. Ou, L. M. Kakutani, J. R. Keeffe, H. J. Wu, M. Howarth, A. P. West, C. O. Barnes, M. C. Nussenzweig, P. J. Bjorkman, Mosaic nanoparticles elicit cross-reactive immune responses to zoonotic coronaviruses in mice. *Science (1979)* **371**, 735–741 (2021).
52. K. W. Ng, N. Faulkner, K. Finsterbusch, M. Wu, R. Harvey, S. Hussain, M. Greco, Y. Liu, S. Kjaer, C. Swanton, S. Gandhi, R. Beale, S. J. Gamblin, P. Cherepanov, J. McCauley, R. Daniels, M. Howell, H. Arase, A. Wack, D. L. V. Bauer, G. Kassiotis, SARS-CoV-2 S2–targeted vaccination elicits broadly neutralizing antibodies. *Sci Transl Med* **14**, 3715 (2022).
53. S. Ravichandran, E. M. Coyle, L. Klenow, J. Tang, G. Grubbs, S. Liu, T. Wang, H. Golding, S. Khurana, Antibody signature induced by SARS-CoV-2 spike protein immunogens in rabbits. *Sci Transl Med* **12**, 3539 (2020).
54. W. Pang, Y. Lu, Y. B. Zhao, F. Shen, C. F. Fan, Q. Wang, W. Q. He, X. Y. He, Z. K. Li, T. T. Chen, C. X. Yang, Y. Z. Li, S. X. Xiao, Z. J. Zhao, X. S. Huang, R. H. Luo, L. M. Yang, M. Zhang, X. Q. Dong, M. H. Li, X. L. Feng, Q. C. Zhou, W. Qu, S. Jiang, S. Ouyang, Y. T. Zheng, A variant-proof SARS-CoV-2 vaccine targeting HR1 domain in S2 subunit of spike protein. *Cell Research 2022 32:12* **32**, 1068–1085 (2022).
55. P. J. Halfmann, S. J. Frey, K. Loeffler, M. Kuroda, T. Maemura, T. Armbrust, J. E. Yang, Y. J. Hou, R. Baric, E. R. Wright, Y. Kawaoka, R. S. Kane, Multivalent S2-based vaccines provide broad protection against SARS-CoV-2 variants of concern and pangolin coronaviruses. *EBioMedicine* **86**, 104341 (2022).

56. Y. Ma, Y. Wang, C. Dong, G. X. Gonzalez, W. Zhu, J. Kim, L. Wei, S. M. Kang, B. Z. Wang, SARS-CoV-2 Spike Stem Protein Nanoparticles Elicited Broad ADCC and Robust Neutralization against Variants in Mice. *Small* **18**, 2200836 (2022).
57. D. T. O'Hagan, G. S. Ott, G. Van Nest, R. Rappuoli, G. Del Giudice, The history of MF59(®) adjuvant: a phoenix that arose from the ashes. *Expert Rev Vaccines* **12**, 13–30 (2013).
58. X. Ma, F. Zou, F. Yu, R. Li, Y. Yuan, Y. Zhang, X. Zhang, J. Deng, T. Chen, Z. Song, Y. Qiao, Y. Zhan, J. Liu, J. Zhang, X. Zhang, Z. Peng, Y. Li, Y. Lin, L. Liang, G. Wang, Y. Chen, Q. Chen, T. Pan, X. He, H. Zhang, Nanoparticle Vaccines Based on the Receptor Binding Domain (RBD) and Heptad Repeat (HR) of SARS-CoV-2 Elicit Robust Protective Immune Responses. *Immunity* **53**, 1315-1330.e9 (2020).
59. P. A.-B. Weidenbacher, M. Sanyal, N. Friedland, S. Tang, P. S. Arunachalam, M. Hu, O. S. Kumru, M. K. Morris, J. Fontenot, L. Shirreff, J. Do, Y.-C. Cheng, G. Vasudevan, M. B. Feinberg, F. J. Villinger, C. Hanson, S. B. Joshi, D. B. Volkin, B. Pulendran, P. S. Kim, A ferritin-based COVID-19 nanoparticle vaccine that elicits robust, durable, broad-spectrum neutralizing antisera in non-human primates. *bioRxiv* , 2022.12.25.521784 (2022).
60. G. Chattopadhyay, R. Varadarajan, Facile measurement of protein stability and folding kinetics using a nano differential scanning fluorimeter. *Protein Science* **28**, 1127–1134 (2019).
61. P. B. McCray, L. Pewe, C. Wohlford-Lenane, M. Hickey, L. Manzel, L. Shi, J. Netland, H. P. Jia, C. Halabi, C. D. Sigmund, D. K. Meyerholz, P. Kirby, D. C. Look, S. Perlman, Lethal Infection of K18- hACE2 Mice Infected with Severe Acute Respiratory Syndrome Coronavirus . *J Virol* **81**, 813–821 (2007).
62. D. A. Mitchison, J. G. Wallace, A. L. Bhatia, J. B. Selkon, T. V. Subbaiah, M. C. Lancaster, A comparison of the virulence in Guinea-pigs of South Indian and British tubercle bacilli. *Tubercle* **41**, 1–22 (1960).

Acknowledgments: NM acknowledges the Prime Minister Research Fellowship for her fellowship (PM/MHRD-20-17303.03). RV is a JC Bose Fellow of DST. DC acknowledges the Council of Scientific and Industrial Research for his fellowship (09/079(2837)/2019-EMR-I). We acknowledge Ms. Simran Srivastava for providing the sarbecoviruses spike constructs.

Funding: This work was funded in part by a grant to RV from the Bill and Melinda Gates Foundation (INV-005948). Funding for infrastructural support was from DST FIST, UGC Centre for Advanced study, MHRD, and the DBT IISc Partnership Program. The funders had no role in study design, data collection and interpretation, or the decision to submit the work for publication.

Author contributions:

Conceptualization: RV, NM

Methodology: RV, NM, SK, RSR, RS, SBJ, MB, DC, SP, RPR, CL, VJ, PMD, AJ, SSSA

Investigation: NM, SK, RSR, RS, SBJ, MB, DC, SP, RPR, CL, VJ,

Visualization: NM, SK, RSR, RS, SBJ, MB, DC, SP, RPR, CL, VJ

Funding acquisition: RV

Project administration: RV

Supervision: RV

Writing – original draft: NM

Writing – review & editing: All authors

Competing interests: A provisional patent application has been filed for the RS2 formulations described in this manuscript. RV, NM, and RS are inventors. RV is a co-founder of Mynvax, RS, SBJ, MB, and SP are employees of Mynvax Private Limited. Other authors declare that they have no competing interests.

Data and materials availability: All data are available in the main text or the supplementary materials.

List of Supplementary Materials

Figure S1. Immunogenicity of RS2 in BALB/c mice.

Figure S2. Comparative immunogenicity of RS2 and Spike in hACE-2 transgenic mice.

Figure S3. Effect of lyophilization on thermal stability of immunogens.

Figure S4. Effect of transient thermal stress on lyophilized RS2 and S2R.

Figure S5. Immunogenicity of RS2 in hamsters.

Figure S6. Cross-reactivity of immunized mice sera to diverse clades of sarbecovirus spikes.

Figures

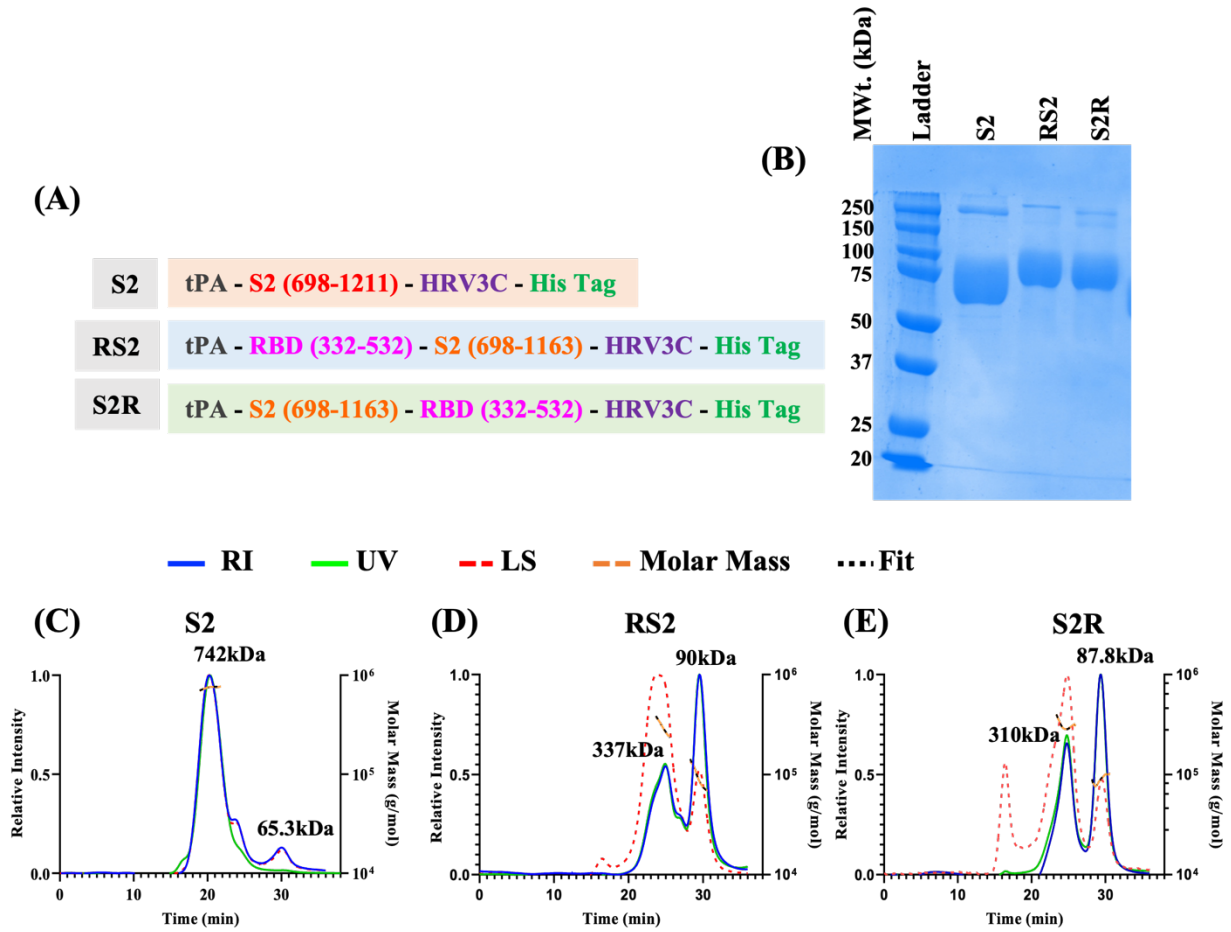

Figure 1. Characterization of S2 and RBD-S2 fusion immunogens. (A) Schematic representation of designed immunogen sequences. **(B)** Reducing SDS-PAGE profile of protein samples. **(C-E)** SEC-MALS profile of purified **(C)** S2, **(D)** RS2 and **(E)** S2R immunogens.

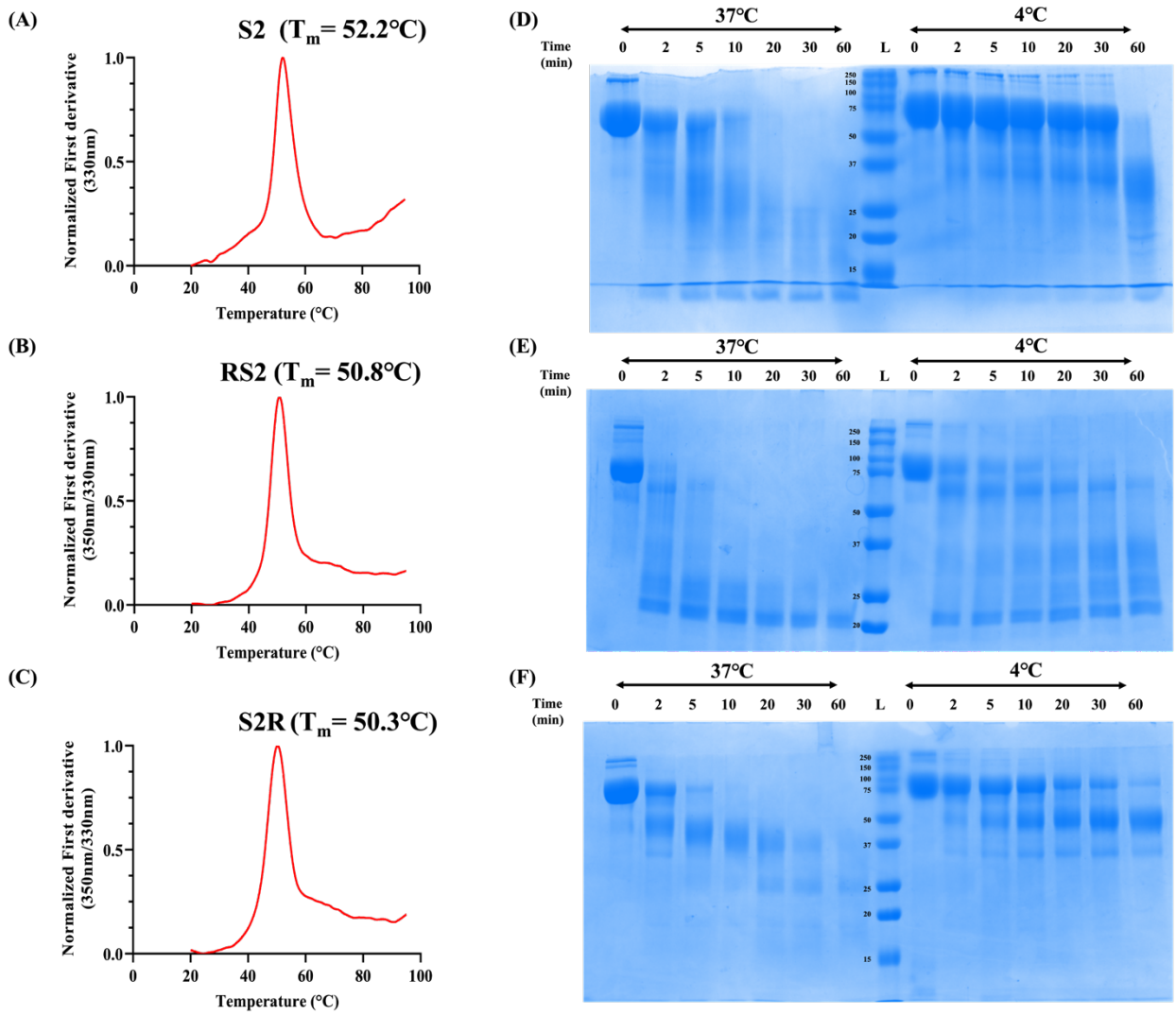

Figure 2. **Equilibrium thermal unfolding and limited trypsin proteolytic profiles of designed immunogens.** Apparent melting temperature of **(A)** S2, **(B)** RS2 and **(C)** S2R were measured using nano-DSF. Coomassie stained SDS-PAGE profile of purified **(D)** S2, **(E)** RS2 and **(F)** S2R subjected to TPCK-Trypsin proteolysis at 37 °C and 4 °C.

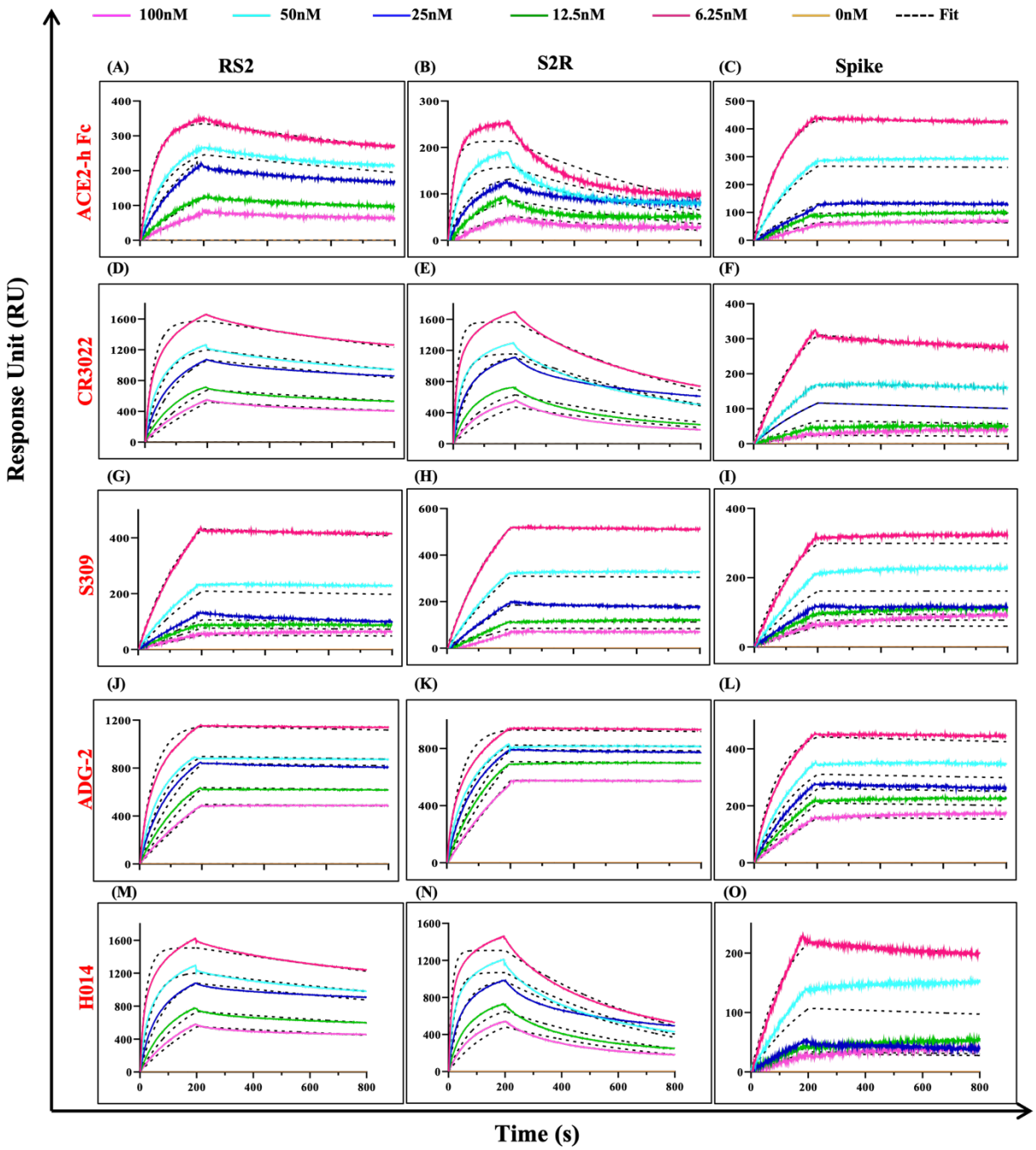

Figure 3. **SPR binding profiles of designed immunogens to RBD specific mAbs.** The binding kinetics of RS2, S2R, and Spike to different RBD conformation-specific ligands **(A-C**) ACE2-hFc, **(D-F)** CR3022, **(G-I)** S309, **(J-L)** ADG-2, and **(M-O**) H014 are shown. No binding was seen to any of these ligands with S2, as expected.

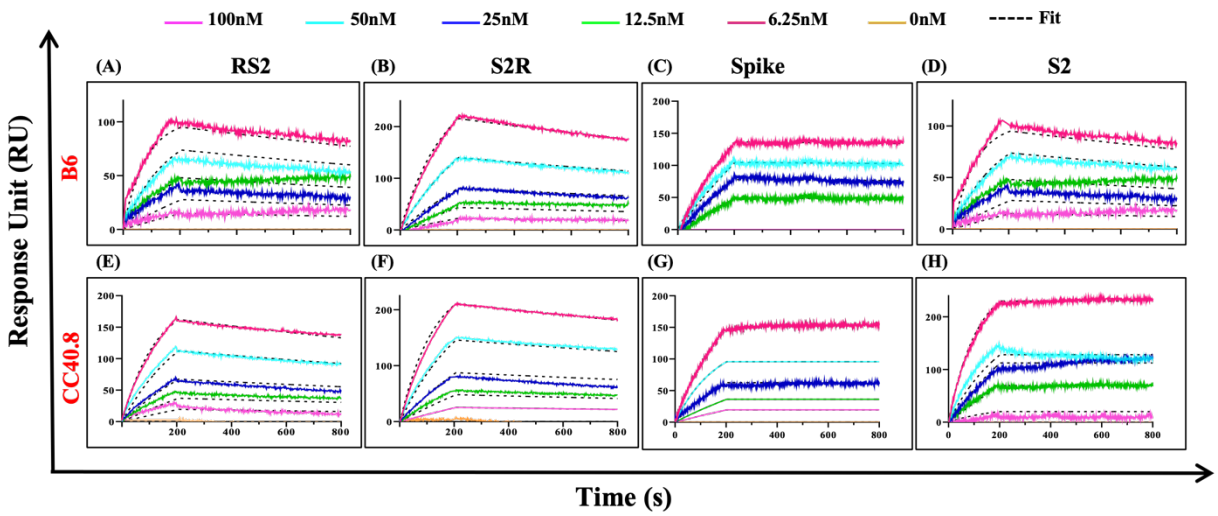

Figure 4. **SPR binding profiles of designed immunogens to S2 specific mAbs.** The binding kinetics of RS2, S2R, Spike and S2 to different S2-specific antibodies **(A-D)** B6, **(E-H)** CC40.8 are shown.

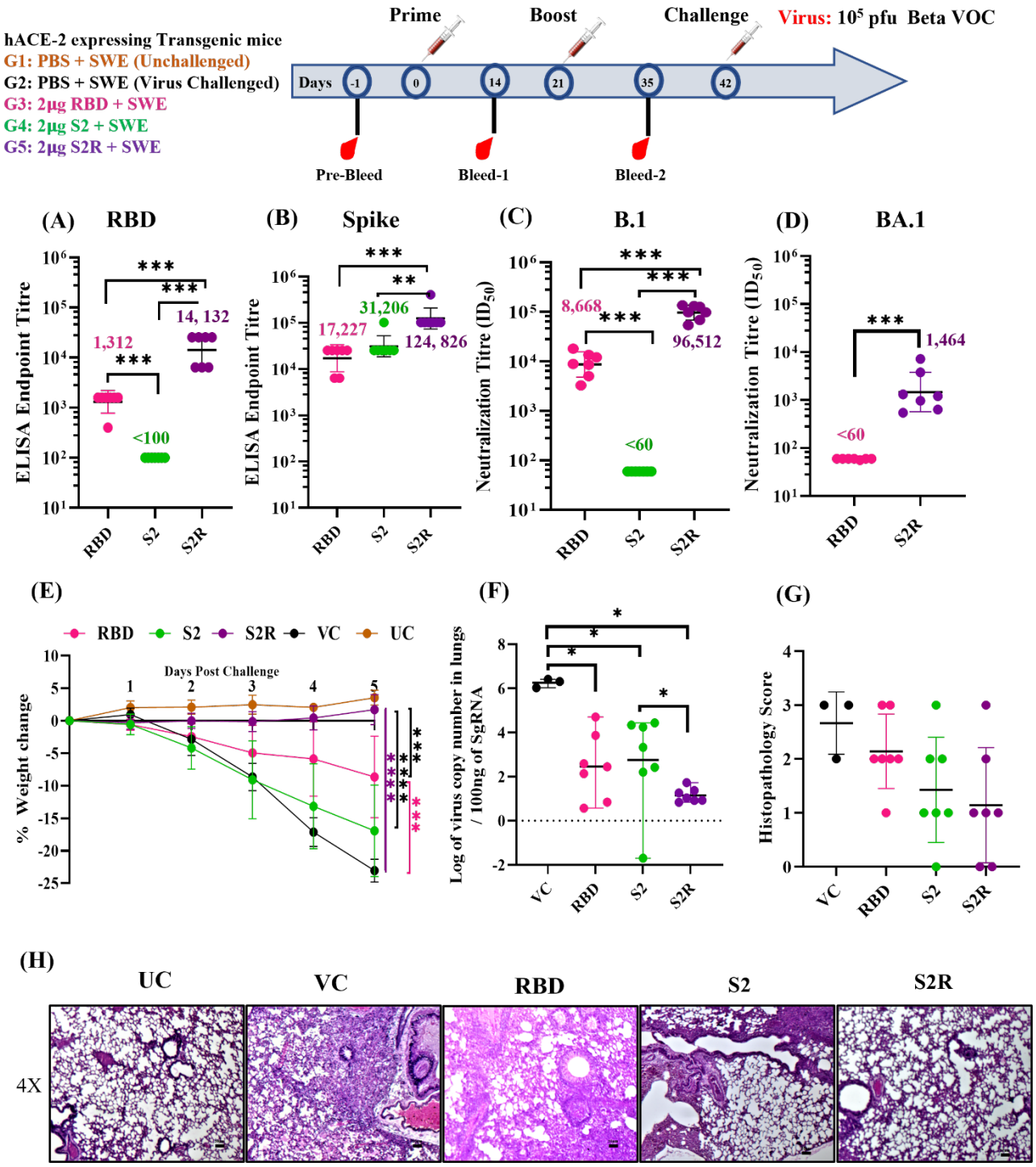

Figure 5. **Immunogenicity of RBD, S2 and S2R in hACE-2 expressing mice.** Three groups of hACE-2 expressing transgenic mice were primed and boosted with 2µg of RBD, S2 and S2R respectively, followed by an intranasal challenge with 10^5 pfu of the beta variant of SARS-CoV-2. **(A and B)** ELISA endpoint titers against RBD and spike ectodomain respectively. **(C and D)** Neutralizing antibody titers elicited by RBD, S2 and S2R against wild type (B.1) and BA.1

Omicron SARS-CoV-2 pseudovirus. No neutralization was seen with S2 immunized animals. **(E)** Lung viral titer. **(F)** Average weight changes up to 5 days post-challenge. **(G)** Histopathology scores of lungs. **(H)** Histology of lung tissue sections from unchallenged control (UC), virus challenged control (VC) and mice immunized with S2R at 4X magnification.

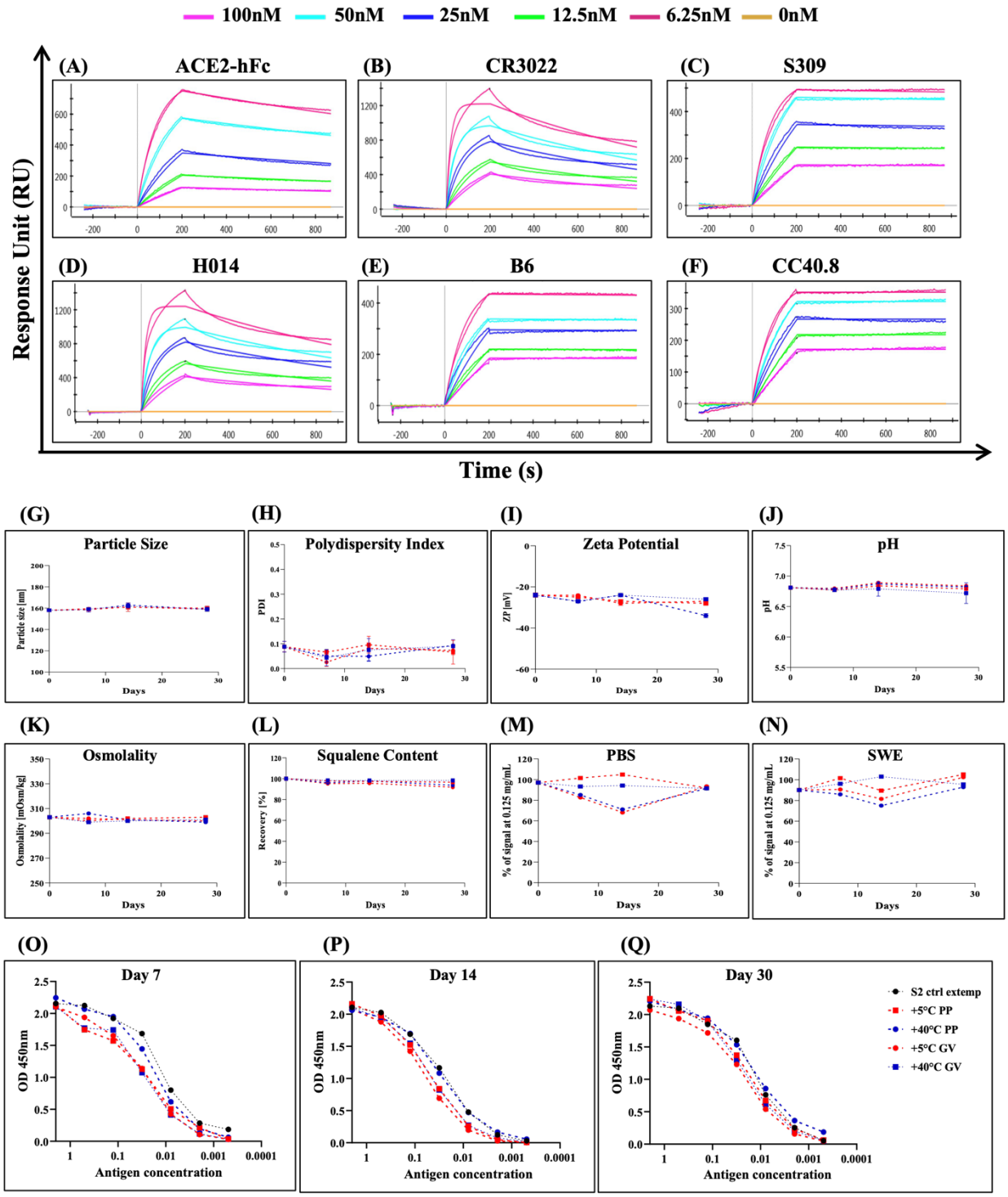

Figure 6. **Stability of RS2.** Characterization of lyophilized and resolubilized RS2 after incubation at 37 °C for 1 month. **(A-F)** Antigenicity of RS2 was monitored using SPR with the following **(A)** ACE2-hFc, **(B)** CR3022, **(C)** S309, **(D)** H014, **(E)** B6 and **(F)** CC40.8. **(G-L)** Physiochemical characterization of RS2 in 1X PBS with equal amount (v/v) of SWE adjuvant incubated at 5 and 40 °C in polypropylene (PP) and glass vials (GV) for one month. Adjuvant properties were measured on day 0, day 7, day 14 and day 30. **(G)** Particle size, **(H)** Polydispersity Index, **(I)** Zeta Potential, **(J)** pH, **(K)** Osmolality, **(L)** Squalene content. **(M and N)** Antigenic integrity of RS2 in PBS and SWE adjuvant was measured based on binding to CR3022 using ELISA. **(O)** Day 7**, (P)** Day 14**, (Q)** Day 30.

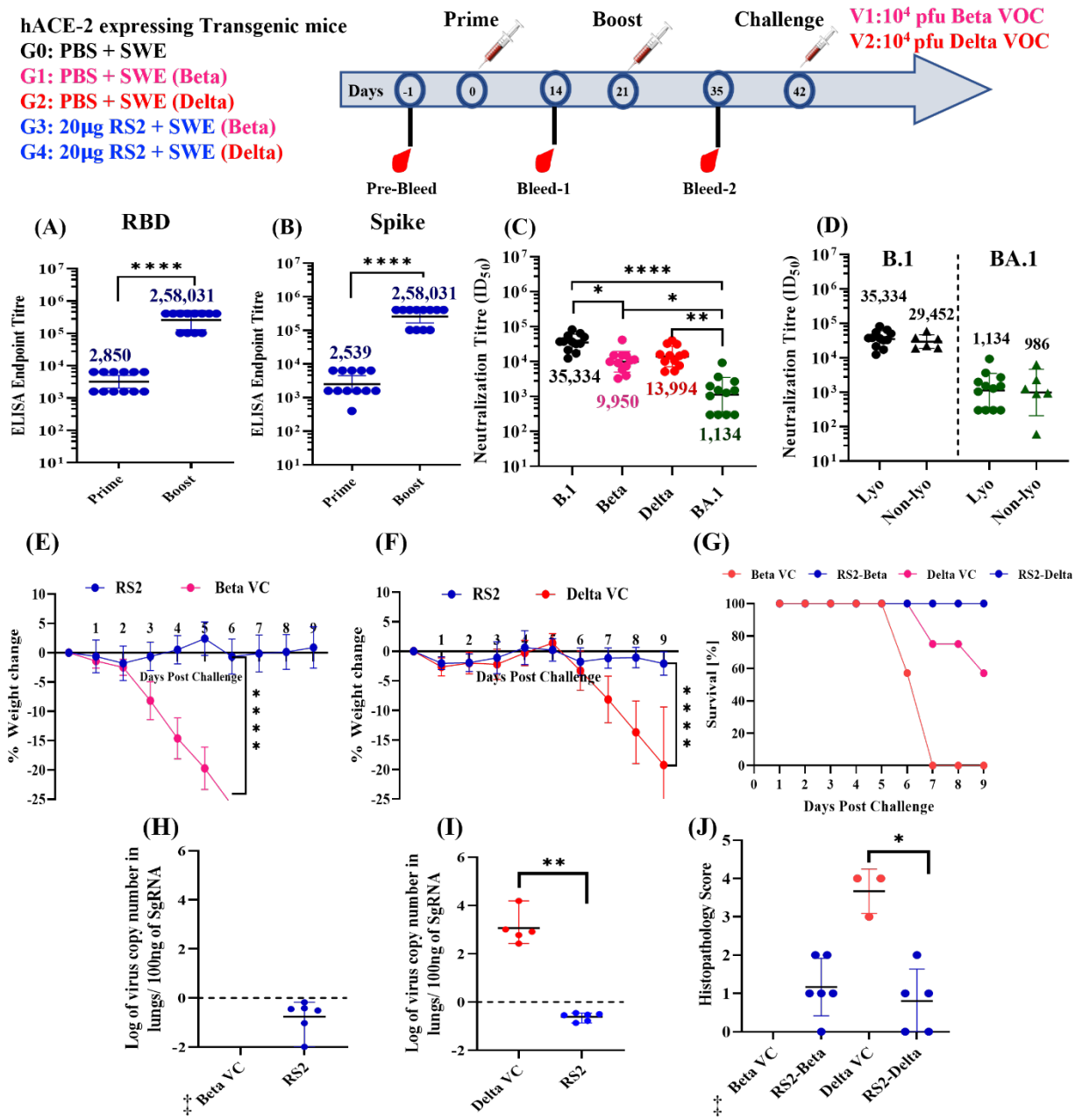

‡ Beta VC: None of the unimmunized mice survived Beta variant challenge

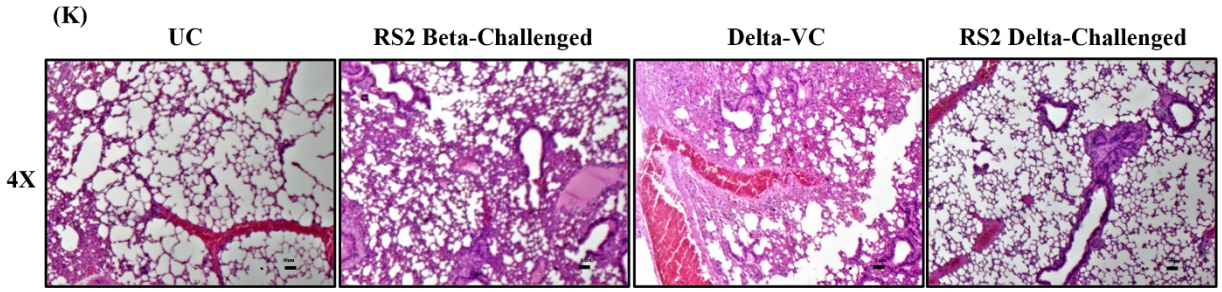

Figure 7. **Immunogenicity of lyophilized RS2 in hACE-2 expressing transgenic mice that had been incubated at 37 °C for 1 month.** hACE-2 expressing transgenic mice immunized twice with 20µg of RS2 that was previously incubated at 37°C for over a month and then formulated in SWE adjuvant. This was followed by intranasal challenge with 10^4 pfu Beta and Delta variants. **(A and B)** ELISA endpoint titers against RBD and spike ectodomain respectively. **(C)** Neutralizing antibody titers against B.1, Beta, Delta and BA.1 pseudoviruses. **(D)** Neutralizing antibody titers elicited by lyophilized RS2 subjected to 37 °C for over a month (Lyo) and non-lyophilized RS2 (Non-lyo) stored at 4 °C against wild type (B.1) and BA.1 Omicron SARS-CoV-2 pseudovirus. Non-lyophilized RS2 data is taken from Fig. S2C and Fig. S2D. **(E and F)** Average weight change upto nine days post-Beta and Delta virus challenge respectively. **(G)** Survival. **(H and I)** Lung viral titers in RS2 immunized mice, challenged with Beta VOC and Delta VOC respectively. **(J)** Histopathology scores of lungs. **(K)** Histology of lung tissue sections from unchallenged control (UC), mice immunized with 20µg RS2 challenged with Beta and Delta variants of SARS-CoV-2, and unvaccinated Delta virus challenged control and at 4X magnification. None of the unvaccinated controls survived the Beta virus challenge.

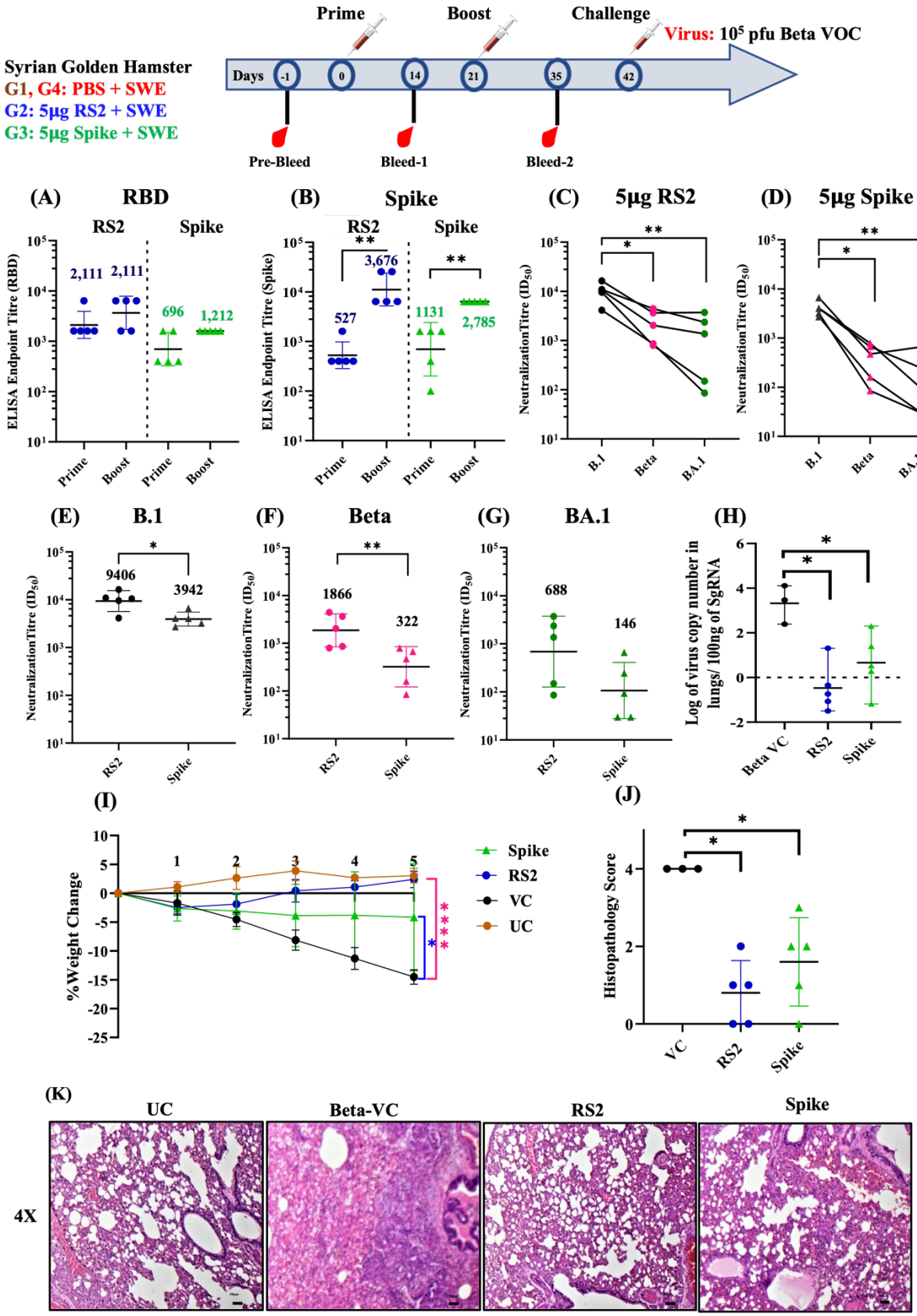
Syrian Golden Hamster
G1, G4: PBS + SWE
G2: 5µg RS2 + SWE
G3: 5µg Spike + SWE
Prime
Boost
Challenge
Virus: 10^5 pfu Beta VOC
Days
-1
0
14
21
35
42
Pre-Bleed
Bleed-1
Bleed-2
(A) RBD
RS2
Spike
ELISA Endpoint Titre (RBD)
2,111
2,111
696
1,212
Prime
Boost
Prime
Boost
(B) Spike
RS2
Spike
ELISA Endpoint Titre (Spike)
527
3,676
1131
2,785
(C) 5µg RS2
Neutralization Titre (ID50)
B.1
Beta
BA.1
(D) 5µg Spike
(E) B.1
9406
3942
RS2
Spike
(F) Beta
1866
322
(G) BA.1
688
146
(H)
Log of virus copy number in lungs/ 100ng of SgRNA
Beta VC
RS2
Spike
(I)
% Weight Change
Spike
RS2
VC
UC
(J)
Histopathology Score
VC
RS2
Spike
(K)
UC
Beta-VC
RS2
Spike
4X

Figure 8. **Comparative protective efficacy of RS2 and spike in hamsters.** Syrian hamsters were immunized twice with 5µg of RS2 or Spike, followed by intranasal challenge with 10^5 pfu of the Beta VOC. **(A and B)** ELISA endpoint titers against RBD and spike ectodomain, respectively. Neutralizing antibody titers against B.1, Beta and Omicron BA.1 pseudoviruses, after immunization with **(C)** RS2 and **(D)** Spike. Comparative neutralizing antibody titers elicited by 5µg of RS2 and spike against **(E)** B.1 **(F)** Beta, and **(G)** Omicron BA.1 pseudovirus. **(H)** Lung viral titer. **(I)** Average weight changes upto five days post-beta variant virus challenge. **(J)** Histopathology scores of lungs. **(K)** Histology of lung tissue sections from unchallenged control (UC), virus challenged control (VC) and hamsters immunized with RS2 and spike at 4X magnification.

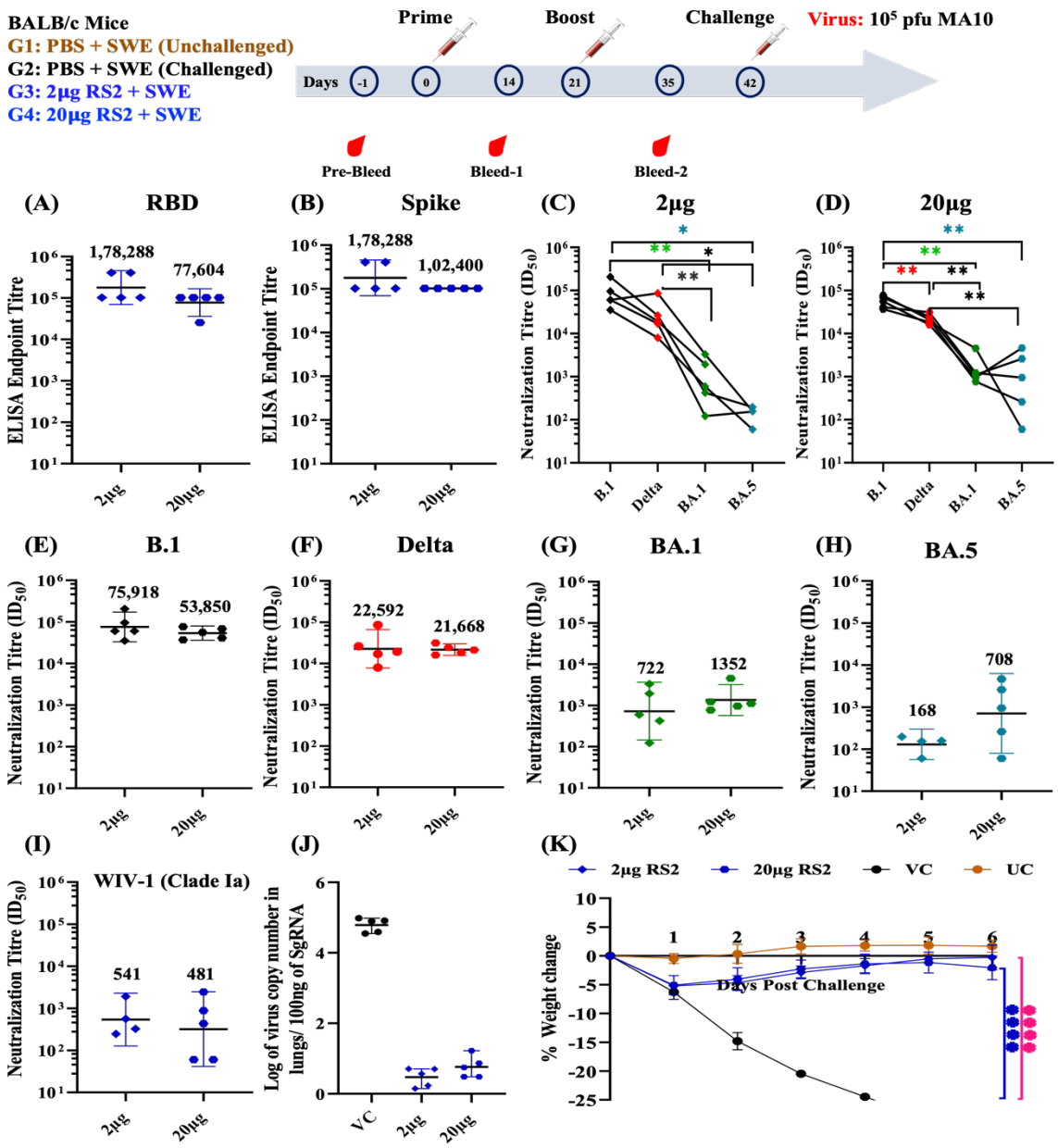

Figure S1. **Immunogenicity of RS2 in BALB/c mice.** BALB/c mice immunized with either 2µg or 20µg RS2 followed by intranasal challenge with 10^5 pfu of MA-10 mouse adapted SARS-CoV-2. **(A and B)** ELISA endpoint titers against RBD and spike ectodomain, respectively. **(C and D)** Neutralizing antibody titers against B.1, Delta, BA.1 and BA.5 pseudoviruses, after immunization with 2 and 20µg doses of RS2. **(E-I)** Neutralizing antibody titers elicited by RS2 against various pseudoviruses. **(J)** Lung viral titers **(K)** Average weight change upto six days post-MA10 challenge.

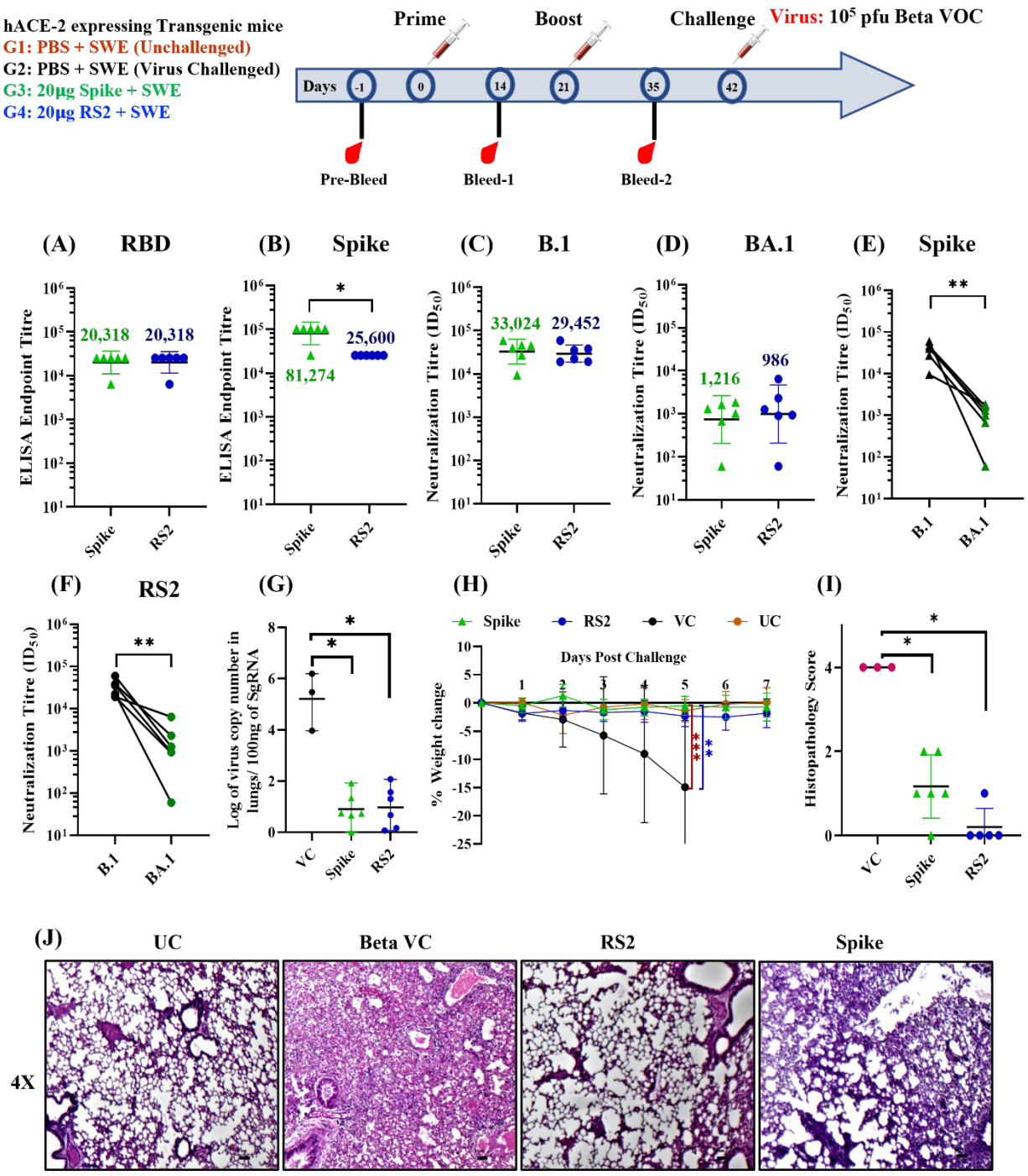

Figure S2. **Comparative immunogenicity of RS2 and Spike in hACE-2 transgenic mice.** Groups of hACE-2 expressing transgenic mice were immunized with 20 µg of RS2 or Spike followed by an intranasal challenge with 10^5 pfu Beta variant of SARS-CoV-2. **(A and B)** ELISA endpoint titers against RBD and Spike ectodomain. Neutralizing antibody titers elicited by RS2

and Spike against **(C)** B.1, and **(D)** BA.1 Omicron pseudovirus. Neutralizing antibody titers against wild type pseudovirus and Omicron pseudovirus, after immunization with **(E)** Spike and **(F)** RS2. **(G)** Lung viral titers. **(H)** Average mice weight changes 7 days post-challenge. **(I)** Histopathology scores of lungs. **(J)** Histology of lung tissue sections from unchallenged control (UC), virus challenged control (VC) and mice immunized with spike and S2R at 4X magnification.

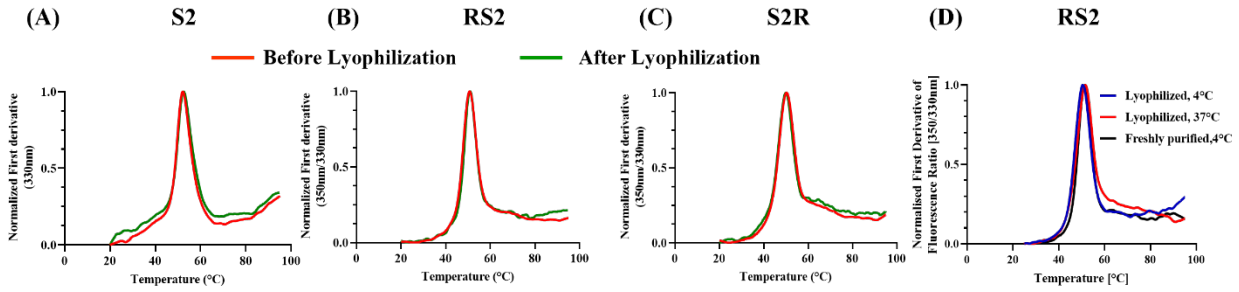

Figure S3. **Effect on thermal stability of lyophilized immunogens.** Equilibrium thermal unfolding profile of **(A)** S2, **(B)** RS2, and **(C)** S2R before and after lyophilization and resolubilization in PBS buffer. **(D)** Thermal stability of lyophilized and resolubilized RS2 after incubation at 37 °C for 1 month.

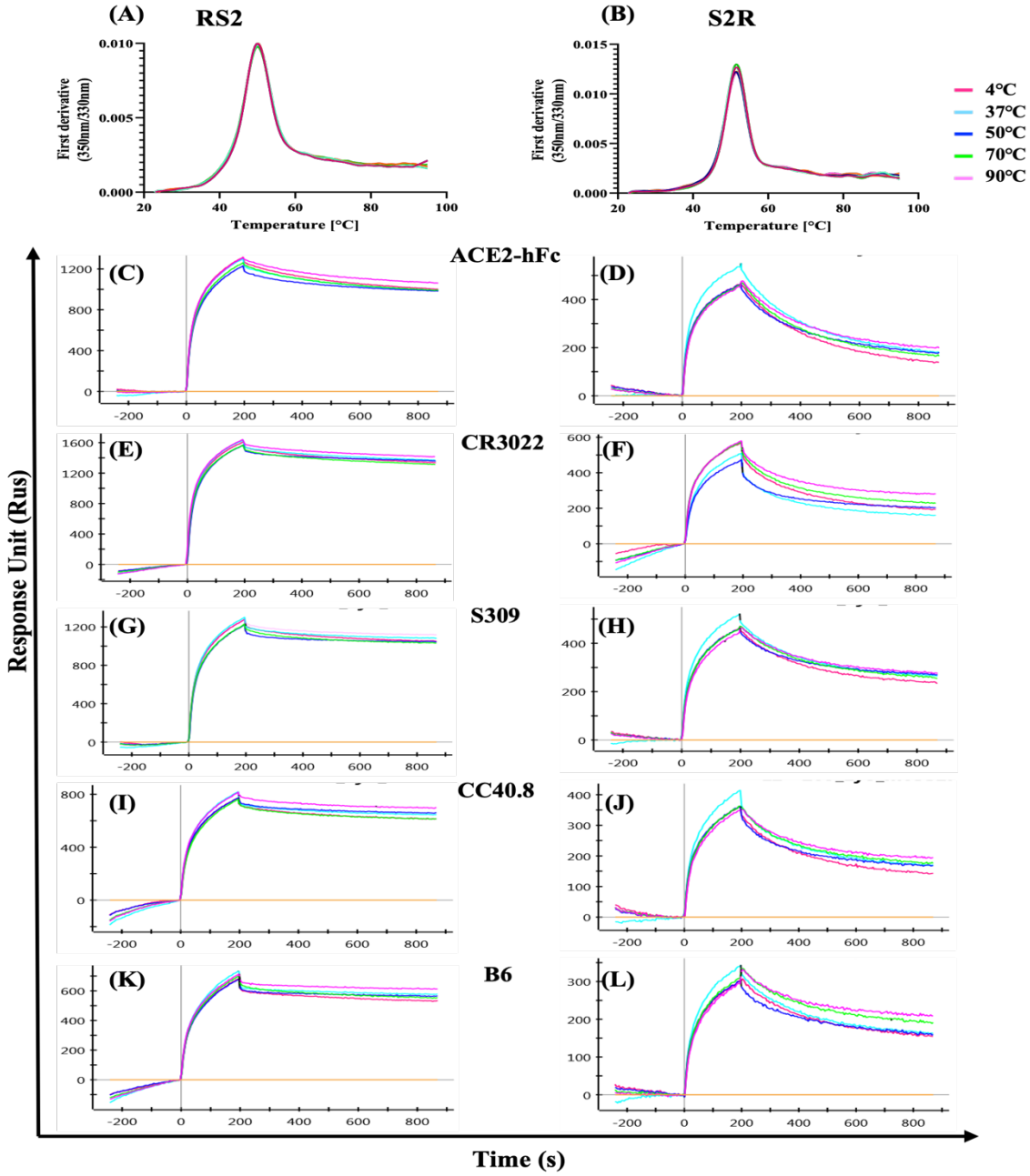

Figure S4. Effect of transient thermal stress on lyophilized RS2 and S2R. Lyophilized RS2 and S2R samples were incubated for one hour at different temperatures (4, 37, 50, 70 and 90 °C). Following reconstitution in PBS buffer thermal stability of **(A)** RS2 and **(B)** S2R was monitored using Nano-DSF. In addition, RS2 and S2R samples were characterized for binding of with panel of RBD (C-H) and S2 (I-L) specific antibodies using SPR **(C-D)** ACE2-hFc, **(E-F)** CR3022, **(G-H)** S309, **(I-J)** CC40.8, and **(K-L)** B6.

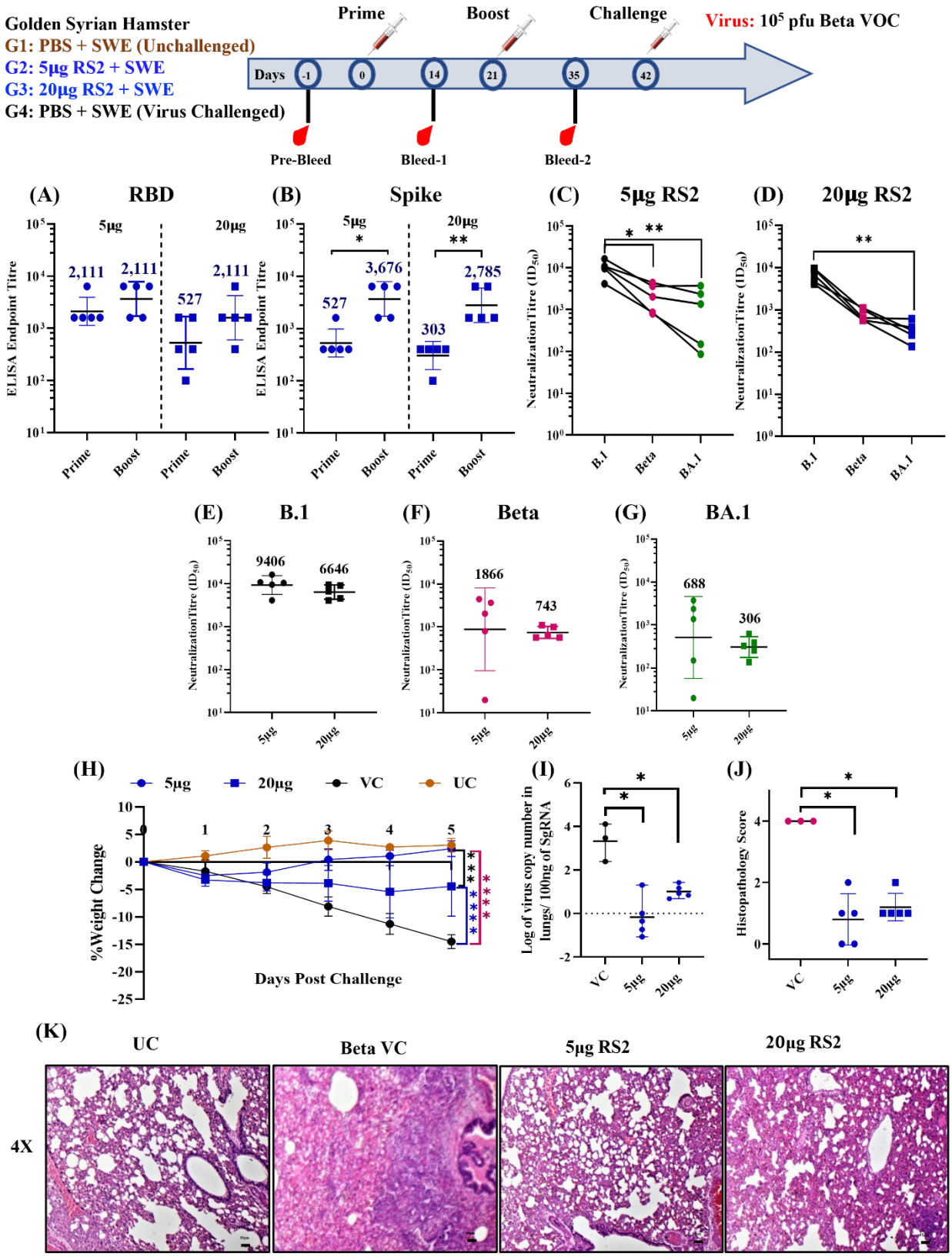
Golden Syrian Hamster
G1: PBS + SWE (Unchallenged)
G2: 5µg RS2 + SWE
G3: 20µg RS2 + SWE
G4: PBS + SWE (Virus Challenged)
Prime
Boost
Challenge
Virus: 10^5 pfu Beta VOC
Days
-1
0
14
21
35
42
Pre-Bleed
Bleed-1
Bleed-2
(A) RBD
(B) Spike
(C) 5µg RS2
(D) 20µg RS2
ELISA Endpoint Titre
Neutralization Titre (ID50)
5µg
20µg
2,111
2,111
527
2,111
527
3,676
303
2,785
Prime
Boost
B.1
Beta
BA.1
(E) B.1
(F) Beta
(G) BA.1
9406
6646
1866
743
688
306
(H)
5µg
20µg
VC
UC
%Weight Change
Days Post Challenge
(I)
Log of virus copy number in lungs/ 100ng of SgRNA
(J)
Histopathology Score
(K)
UC
Beta VC
5µg RS2
20µg RS2
4X

Figure S5. Immunogenicity of RS2 in hamsters. Syrian hamsters immunized twice with 5 or 20µg RS2 followed by intranasal challenge with 10^5 pfu Beta variant. **(A and B)** ELISA endpoint titers against RBD and spike ectodomain, respectively. **(C and D)** Neutralizing antibody titers against B.1, Beta and BA.1 pseudoviruses, after immunization with 5 and 20µg doses of RS2. Neutralizing antibody titers elicited by 5 and 20µg of RS2 against **(E)** B.1 **(F)** Beta, and **(G)** BA.1 pseudovirus. **(H)** Average hamster weight change, 5 days post-Beta variant virus challenge. **(I)** Lung viral titers. **(J)** Histopathology scores of lungs. **(K)** Histology of lung tissue sections from unchallenged control (UC), virus challenged control (VC) and hamster immunized with 5µg RS2 and 20µg RS2 at 4X magnification.

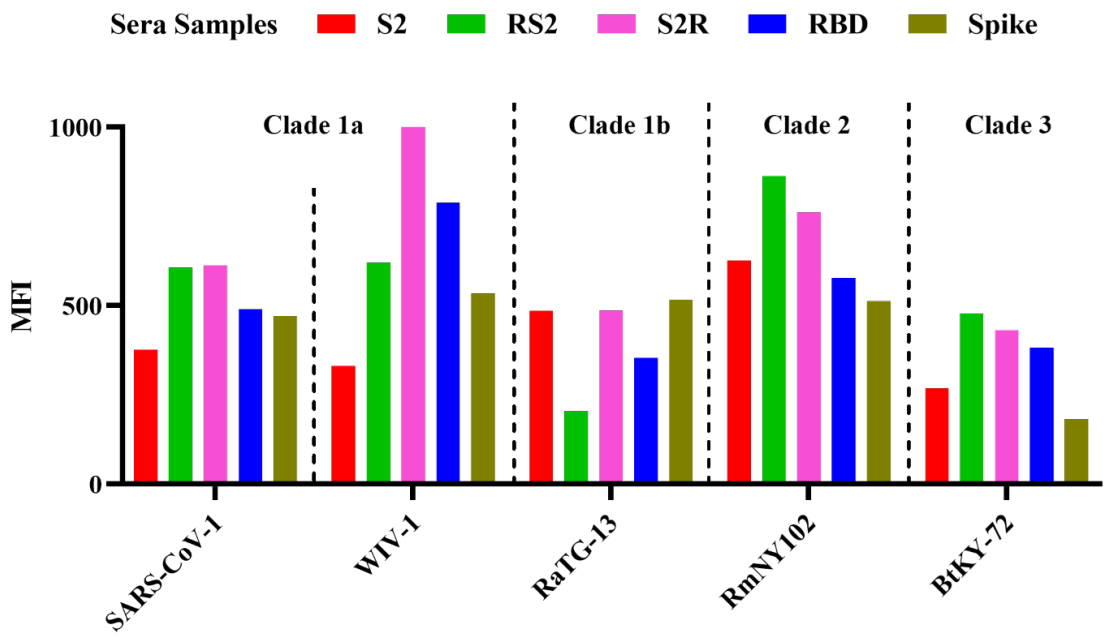

Figure S6. Cross-reactivity of immunized mice sera to diverse clades of sarbecovirus spikes. Sarbecovirus spike specific IgG antibodies were quantified in RBD, S2, RS2, S2R and Spike immunized mice sera. HEK-293 cells expressing different full length sarbecovirus spike constructs were incubated with 1:100 diluted different sera samples obtained from mice immunized with RBD, S2, RS2, S2R and Spike for 30 min. After washing, samples were labelled with anti-mouse Alexa Fluor 633 (1:1200) for 30 min. Samples were washed and then analyzed using a BD Aria III instrument. Median fluorescence intensity (MFI) was calculated as follows: MFI of HEK-293 cells expressing spike – MFI of HEK cells alone.

Ligand	Parameter	Immunogens		
		RS2	S2R	Spike
ACE2-hFc	k_a ($M^{-1}s^{-1}$)	$2.30 \pm 0.01\times10^{5}$	$5.15 \pm 0.10\times10^{5}$	$1.07 \pm 0.01\times10^{5}$
	k_d (s^{-1})	$3.90 \pm 0.02\times10^{-4}$	$1.49 \pm 0.01\times10^{-3}$	$3.04 \pm 0.07\times10^{-5}$
	K_D (M)	$1.71 \pm 0.01\times10^{-9}$	$2.99 \pm 0.06\times10^{-9}$	$2.88 \pm 0.16\times10^{-10}$
CR3022	k_a ($M^{-1}s^{-1}$)	$3.43 \pm 0.02\times10^{5}$	$6.57 \pm 0.07\times10^{5}$	$6.17 \pm 0.11\times10^{4}$
	k_d (s^{-1})	$4.13\pm 0.03\times10^{-4}$	$1.39 \pm 0.01\times10^{-3}$	$2.45 \pm 0.05\times10^{-4}$
	K_D (M)	$1.21\pm 0.01\times10^{-9}$	$2.15 \pm 0.03\times10^{-9}$	$4.06 \pm 0.11\times10^{-9}$
S309	k_a ($M^{-1}s^{-1}$)	$5.78 \pm 0.08\times10^{4}$	$5.31 \pm 0.05\times10^{4}$	$7.61 \pm 0.13\times10^{4}$
	k_d (s^{-1})	$9.87\pm 0.26\times10^{-5}$	ND*	ND*
	K_D (M)	$1.73\pm 0.05\times10^{-9}$	ND*	ND*
ADG-2	k_a ($M^{-1}s^{-1}$)	$2.17 \pm 0.01\times10^{5}$	$2.26 \pm 0.01\times10^{5}$	$1.36 \pm 0.01\times10^{5}$
	k_d (s^{-1})	$4.51\pm 0.23\times10^{-5}$	ND*	$6.88 \pm 0.06\times10^{-5}$
	K_D (M)	$1.05\pm 0.05\times10^{-10}$	ND*	$5.10 \pm 0.20\times10^{-10}$
H014	k_a ($M^{-1}s^{-1}$)	$4.52 \pm 0.03\times10^{5}$	$7.82 \pm 0.05\times10^{5}$	$7.38 \pm 0.13\times10^{5}$
	k_d (s^{-1})	$3.49 \pm 0.03\times10^{-4}$	$1.64 \pm 0.01\times10^{-3}$	$1.66 \pm 0.05\times10^{-4}$
	K_D (M)	$7.78 \pm 0.08\times10^{-10}$	$2.14 \pm 0.03\times10^{-9}$	$2.30 \pm 0.08\times10^{-9}$

Table S1: Kinetic parameters of RS2, S2R, and Spike for binding to different RBD conformation-specific ligands in PBS pH 7.4 at 25 ºC. ND*: No dissociation.

Ligand	Parameter	Immunogens			
		RS2	S2R	Spike	S2
B6	k_a ($M^{-1}s^{-1}$)	$2.53 \pm 0.05\times10^{5}$	$1.24 \pm 0.01\times10^{5}$	$3.16 \pm 0.07\times10^{4}$	$2.04 \pm 0.07\times10^{5}$
	k_d (s^{-1})	$7.32 \pm 0.36\times10^{-4}$	$1.53 \pm 0.8\times10^{-3}$	$3.48 \pm 0.25\times10^{-5}$	$2.50 \pm 0.25\times10^{-4}$
	K_D(M)	$2.30 \pm 0.12\times10^{-9}$	$1.24 \pm 0.12\times10^{-8}$	$1.12 \pm 0.08\times10^{-9}$	$1.22 \pm 0.08\times10^{-9}$
CC40.8	k_a ($M^{-1}s^{-1}$)	$1.62 \pm 0.01\times10^{5}$	$1.62 \pm 0.02\times10^{5}$	$1.19 \pm 0.02\times10^{5}$	9.11×10^{4}
	k_d (s^{-1})	$6.77 \pm 0.01\times10^{-4}$	$5.30 \pm 1.6\times10^{-4}$	ND*	ND*
	K_D (M)	$4.22 \pm 0.08\times10^{-9}$	$3.23 \pm 0.03\times10^{-9}$	ND*	ND*

Table S2: Kinetic parameters of S2, RS2, S2R, and Spike for binding to different S2-specific ligands in PBS pH 7.4 at 25 ºC. ND*: No dissociation.

Ligand	k_a ($M^{-1}s^{-1}$)	k_d (s^{-1})	K_D (M)
ACE-2hFc	$1.2 \pm 0.01\times10^{5}$	$3.2 \pm 0.01\times10^{-4}$	$2.7 \pm 0.01\times10^{-9}$
CR3022	$4.8 \pm 0.01\times10^{5}$	$7.9 \pm 0.4\times10^{-4}$	$1.6 \pm 0.01\times10^{-9}$
S309	$1.2 \pm 0.01\times10^{5}$	$3.2 \pm 0.01\times10^{-5}$	$2.4 \pm 0.01\times10^{-10}$
H014	$5.0 \pm 0.01\times10^{5}$	$6.8 \pm 0.4\times10^{-4}$	$1.3 \pm 0.01\times10^{-9}$
B6	$1.1 \pm 0.01\times10^{5}$	$1.6 \pm 0.01\times10^{-5}$	$1.2 \pm 0.01\times10^{-10}$
CC40.8	$1.1 \pm 0.01\times10^{5}$	ND*	ND*

Table S3: Kinetic parameters for binding of lyophilized and resolubilized RS2 after incubation at 37 ºC for 1 month to different RBD-specific and S2-specific ligands in PBS pH 7.4 at 25 ºC. ND*: No dissociation.